STRUCTURAL ANALYSIS AND FINITE ELEMENT MODELING OF ALUMINUM HONEYCOMB SANDWICH STRUCTURES

Maimouna Doukoure

Thesis Prepared for the Degree of

MASTER OF SCIENCE

UNIVERSITY OF NORTH TEXAS

May 2021

APPROVED:

Cheng Yu, Major Professor
Leticia H. Anaya, Committee Member
Saman Rashidyan, Committee Member
Kuruvilla John, Chair of the Department of Mechanical Engineering
Hanchen Huang, Dean of the College of Engineering
Victor Prybutok, Dean of the Toulouse Graduate School

Doukoure, Maimouna. *Structural Analysis and Finite Element Modeling of Aluminum Honeycomb Sandwich Structures*. Master of Science (Engineering Technology), May 2021, 70 pp., 13 tables, 44 figures, 38 numbered references.

The objective of this research is to determine how the sandwich's physical characteristics have an impact on the mechanical properties, determine under what conditions the specimens will be lighter and mechanically stronger, and determine if the use of an aluminum honeycomb sandwich as a construction material is feasible. The research has aimed at the use of aluminum sandwiches as light and strong material. The study of the structural layers' damage resistance and tolerance demonstrated that the top and bottom layers play a crucial role. The thesis presents three test results from aluminum honeycomb sandwich compression horizontal, compressive vertical, and bending tests. Also, each group was displayed mechanically and simulated in Abaqus. The study determines the mechanical properties such as maximum elastic stress-strain, ultimate stress-strain, fracture point, density, poison ration, young modulus, and maximum deflection was determined. The energy absorbed by the FEA, such modulus of elasticity, resilience, and toughness, the crack propagation, the test's view shows aluminum honeycomb behaved like a brittle material with both compression test. And the maximum deflection, crack propagation, shear forces, bending moment, and images illustrated that the layers play a crucial role in the 3-point bend test.

ACKNOWLEDGMENTS

I want to express my deepest gratitude to my advisor Dr. Yu, for providing genius instruction, motivation, a vision that inspired me. Also, to my committee members Dr. Anaya Leticia and Dr. Saman Rashidyan, for the initial support mastermind knowledge, make this work happen. Special thanks to the sponsor, the United States Army. My sincere gratitude goes to the UNT Department of Mechanical Engineering for my teaching and training.

I want to express my gratitude toward my family for the encouragement that helped me complete this paper, especially to my caring, loving, and supportive husband BB and children Lamarana, Mariam and Asmaou, my deepest gratitude. I am incredibly grateful to my parent for their love, caring, and sacrifices for preparing my future.

TABLE OF CONTENTS

Page

ACKNOWLEDGMENTS iii

LIST OF TABLES vi

LIST OF FIGURES vii

CHAPTER 1. INTRODUCTION 1

CHAPTER 2. LITERATURE REVIEW 4

2.1 Origin and Properties of Aluminum Honeycomb Sandwich 4

2.2 Aluminum Honeycomb Sandwich Manufacturing 6

2.3 Aluminum Honeycomb Sandwich application 8

2.4 Advantages of Aluminum Honeycomb Sandwich in Cold-Formed Steel (CFS)… 10

2.5 Finite Element Analysis 12

CHAPTER 3. THESIS STATEMENT 18

CHAPTER 4. RESEARCH METHODOLOGY 19

4.1 Mechanical Properties of Aluminum 19

4.2 Engineering Stress-Strain 20

4.3 True Stress-Strain 22

4.4 Compressive Test 24

4.5 Compression Vertical of Aluminum Honeycomb Sandwich Set-Up 25

4.5.1 Mechanical Test 25

4.5.2 Abaqus Simulation 25

4.6 Compression Horizontal of Aluminum Honeycomb Sandwich Set-Up 26

4.6.1 Mechanical Test 26

4.6.2 Abaqus Simulation 27

4.7 Bending Test 27

4.7.1 Mechanical Test of Aluminum Honeycomb Sandwich 3-Point Bend Set-Up 29

4.7.2 Abaqus Simulation of Aluminum Honeycomb Sandwich 3-Point Bend Set-Up 29

4.7.3 Compressive Vertical Displacement 30

CHAPTER 5. EXPECTED RESEARCH RESULTS 31

5.1 Compression Test 31

5.1.1 Compressive Vertical Displacement 32

5.1.2 Properties Mechanic of the Honeycomb Sandwich with Compression Vertical 35

5.2 Compressive Horizontal of the Aluminum Honeycomb Sandwich 44

5.2.1 Properties Mechanic of the Aluminum Honeycomb Sandwich with Compression Horizontal 47

5.3 Three-Point Bending Test of the Aluminum Honeycomb Sandwich 57

5.3.1 Maximum of Deflection of the Aluminum Honeycomb Sandwich 3-Point Bend 59

5.3.2 Maximum Bending Moment and Shear Forces of the Aluminum Honeycomb Sandwich 63

CHAPTER 6. CONCLUSION 67

REFERENCES 69

LIST OF TABLES

Page

Table 4.1: The mechanical properties of the aluminum honeycomb 20

Table 4.2: Engineering stress-strain of the aluminum 21

Table 4.3: True stress-strain of the aluminum 22

Table 4.4: Honeycomb sandwich layers dimensions in compression 25

Table 4.5: Honeycomb sandwich layers dimensions in bending test 28

Table 5.1: Modulus of elasticity and resilience with the compressive vertical 38

Table 5.2: Ultimate stress and strain with the compressive vertical 39

Table 5.3: Modulus of the toughness for the compressive vertical 43

Table 5.4: Modulus of elasticity and resilience with the compressive horizontal 51

Table 5.5: Ultimate stress and strain with the compressive horizontal 51

Table 5.6: Modulus of the toughness of the compressive horizontal 56

Table 5.7: Mechanical properties of the 3-point data 62

Table 5.8: Maximum shear forces and bending moment 66

LIST OF FIGURES

Page

Figure 1.1: Analysis of aluminum honeycomb sandwich in Abaqus 3

Figure 2.1: Examples of cellular materials 5

Figure 2.2: Aluminum panel for buildings 10

Figure 2.3: Five stages of completing finite element analysis 17

Figure 4.1: Comparison of the plots between the engineering stress-strain and true stress strain 23

Figure 4.2: Honeycomb sandwich 24

Figure 4.3: Compression vertical testing set-up of INSTRON-4482C4859 machine 25

Figure 4.4: Compressive vertical of the honeycomb sandwich loaded at the top layer 26

Figure 4.5: Compression horizontal testing set-up of INSTRON-4482C4859 machine 26

Figure 4.6: Compressive horizontal of the honeycomb sandwich loading 27

Figure 4.7: Honeycomb layers 28

Figure 4.8: Test fixture on test resource machine for the three-point bend 29

Figure 4.9: Three points bend set in Abaqus 30

Figure 5.1: Compression vertical of S1, S2, and S3 33

Figure 5.2: Compressive vertical simulation of the honeycomb 33

Figure 5.3: Plots with Abaqus and mechanical tests with compression vertical 34

Figure 5.4: Modulus resilience of Sample 1 35

Figure 5.5: Modulus resilience of Sample 2 36

Figure 5.6: Modulus resilience of Sample 3 37

Figure 5.7: Abaqus simulation with Node 452 elastic modulus 38

Figure 5.8: The modulus of toughness of Sample 1 40

Figure 5.9: The modulus of toughness of Sample 2 41

Figure 5.10: The modulus of toughness of Sample 3 42

Figure 5.11: The modulus of toughness of the in Abaqus with Node 452 42
Figure 5.12: Compression horizontal of samples S4, S5 and S6 45
Figure 5.13: Compressive horizontal simulation of the honeycomb sandwich 45
Figure 5.14: Plots with Abaqus and mechanical tests with compression horizontal 46
Figure 5.15: Modulus resilience of Sample 4 47
Figure 5.16: Modulus resilience of Sample 5 48
Figure 5.17: Modulus resilience of Sample 6 49
Figure 5.18: Modulus resilience of Node 1151 50
Figure 5.19: Modulus toughness of S4 52
Figure 5.20: Modulus toughness of S5 53
Figure 5.21: Modulus toughness of S6 54
Figure 5.22: Modulus toughness of Node 1151 55
Figure 5.23: Mechanical test of the 3-point bend 58
Figure 5.24: Abaqus simulation of the 3-point bend test 58
Figure 5.25: Plots with Abaqus and mechanical tests with compression horizontal 59
Figure 5.26: Bend 1 elastic displacement 60
Figure 5.27: Bend 2 elastic displacement 61
Figure 5.28: Abaqus simulation elastic displacement 62
Figure 5.29: Analysis of shear forces and bending moment diagram in Abaqus 64
Figure 5.30: Analysis of shear forces and bending moment diagram with Bend Test 1 65
Figure 5.31: Analysis of shear forces and bending moment diagram with Bend Test 2 65

CHAPTER 1

INTRODUCTION

Since the earliest prehistoric man learned how to build a shelter, humans used the natural environment, such as trees, hay, to get minimum protection from the cold and the rain. Since then, humans have tried to develop their living place by modeling and optimizing material construction to achieve higher shelter quality. Our goal is to use an aluminum honeycomb sandwich as a construction material to determine its affiance for building material.

Scientists and engineers try to improve the quality of the construction material by optimizing the construction material. So, the engineering requirement and development of a concept need to consider the choice, the design of the construction material such as metal, wood, metal, concrete, and more.

This research presented three sets of aluminum honeycomb sandwich results: the compression horizontal, compressive vertical, and three-point bending tests. Furthermore, each group was displayed mechanically and simulated in Abaqus. The test data identified the mechanical properties such as modulus of stress-strain, ultimate stress-strain, fracture point, density, poison ration, the Young modulus, the maximum displacement, forces, and maximum deflection. Moreover, the energy absorbed defined the modulus of elasticity, resilience, and toughness.

The aluminum honeycomb sandwich is a cellular structure resembling beehives (hexagonal) and face-sheets. In general, the material is an assembly of three layers: the top layer, the bottom layer, and the honeycomb layer inserted between two thin panels of aluminum (top and bottom layers) for illustration refer to Figure I. 1. The aluminum honeycomb sandwich is light and strong, as determined by the yield strength in mechanical properties.

The aluminum honeycomb sandwich has many advantages as well as disadvantages. Some of the benefits of aluminum honeycomb sandwich are versatile enough to work in many different areas (e.g., sound absorption, fragmentation fracture, impact absorption, heat sinks, exchange, energy-saving, high impact resistance, vibration damping, and recyclable).

The aluminum honeycomb sandwich's primary disadvantage lies in the difficulty of achieving an excellent interfacial attachment between the honeycomb and the layers (top and bottom layers) during the manufacturing. Also, the temperature and fusion bonding must be managed for a better product. Aluminum honeycomb sandwich can have corrosion problems in contact with the salted-water environment (marine boat). The honeycomb sandwich deformation is irreversible when impacted.

Aluminum honeycomb sandwich used to specific markets (e.g., military, aeronautics, construction, transportation, and automotive as a structural material or interior panel.) In general, honeycomb sandwich metallic structures have an outstanding advantage in some applications (e.g., sound absorption, fragmentation fracture, impact absorption, heat sinks, heat exchangers, etc.). The use of cold-foamed steel (CFS) framing techniques can reduce aluminum sandwich manufacturing in multiple ways by optimizing metal production and reducing waste quantity.

Several scientists and engineers have tried to improve the quality of the aluminum to create a honeycomb base. For instance, they simulated naturally porous materials (e.g., bee comb, bone, cord, and coral) based on the repeating internal geometry faces or edges. These simulation techniques extended to the production of aluminum honeycomb sandwich manufacturing. Even though the manufacturing of aluminum honeycomb sandwich was improved using computerized tones, the fusion bonding temperature is still tricky to controlled.

This thesis intends to address the above problem by studying aluminum honeycomb

sandwiches' behavior using Finite Element Analysis (FEA) in Abacus and the mechanical test. The use of FEA for engineering design allows humans to solve previously unsolved problems.

This research proposes adding another modern simulation software tool, Abacus, to test the aluminum sandwich prototypes for compression vertical and horizontal. Other software tools in the market for FEA are Polyval, Agros 2D, ANSA Preprocessor, CalculiX, DIANA FEA, Deal.II, Dune, Elmer, etc.

Abaqus will be used for this research paper to solve and compute relevant quantities of the honeycomb sandwich structure (stress, strain) and investigate the sandwich structure under given loads. For an example of an FEA analysis, refer to Figure 1.2.

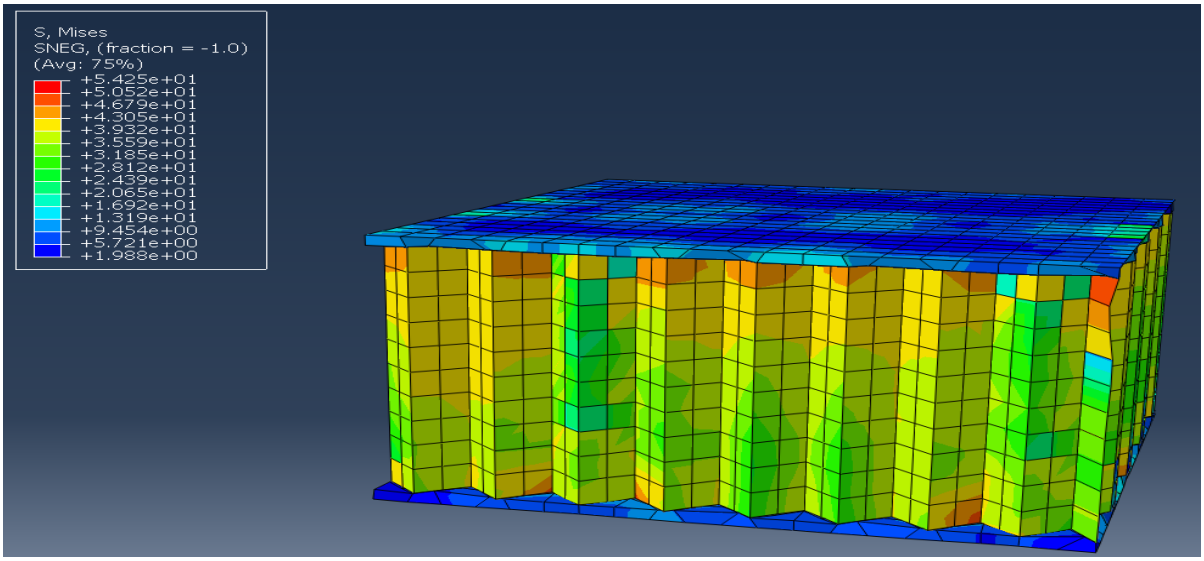

Figure 1.1: Analysis of aluminum honeycomb sandwich in Abaqus

CHAPTER 2

LITERATURE REVIEW

2.1 Origin and Properties of Aluminum Honeycomb Sandwich

Aluminum founded in the earth undergoes the following stages: aluminum ore, mined aluminum, refined aluminum (bauxite), and smelted aluminum [9]. T. Dennis Claar et al. (2000) stated that aluminum is the third most used metal after iron and steel. “Aluminum is also the most abundant metal in the earth’s crust and the third most abundant element after oxygen and silicon” [1]. Aluminum is a vital component of almost every part of our human lives. It used in building materials, vehicles that we drive, packaging our foods, etc. The first building in which aluminum was widely used as the Empire State Building in New York, built-in 1931 [36]. According to Azom (2002), aluminum was not discovered until 1809, when an English chemist, Sir Humphry Davy, formally identified and named it.

Most aluminum is alloyed with other elements. Aluminum is at its most versatile when it is combined with other metals to form aluminum alloys. By fusing the aluminum, mechanical properties (e.g., hardness and strength) can be improved. The alloying process gives aluminum excellent properties to suit a range of applications. “Common aluminum alloys are aluminum-manganese (used in beverage containers), aluminum-magnesium (used in appliances and utensils), aluminum-magnesium-silicon (used in buildings and vehicles), and aluminum-copper (used in aircraft)” [9].

Today, aluminum is regularly used in the construction of high-rise buildings and bridges. The lightweight aluminum makes it easier, faster, and more convenient to work with, and it is economical. A building constructed of steel would require much deeper foundations compare to aluminum. Because of the added weight, the cost of the construction can augment.

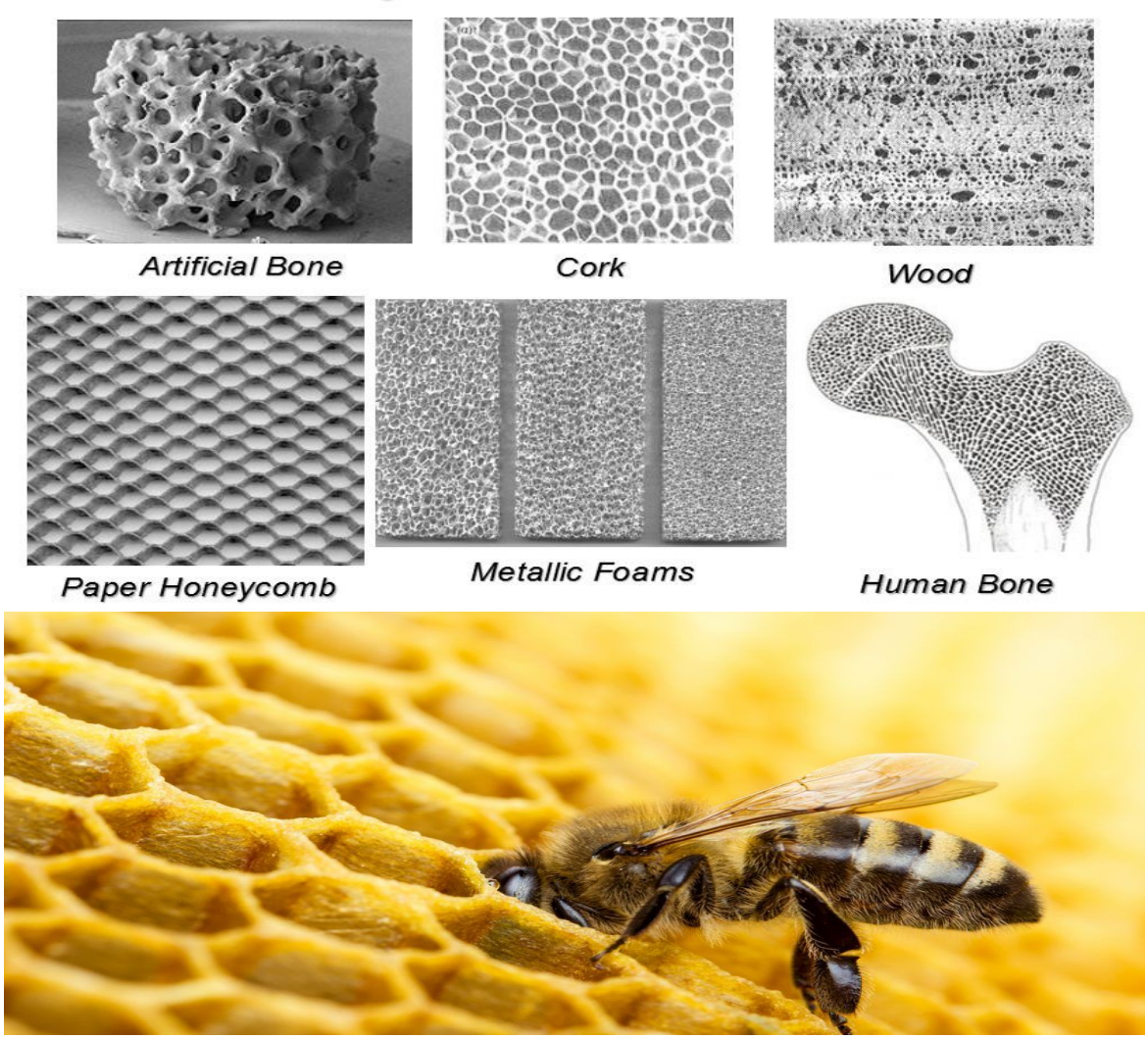

Figure 2.1: Examples of cellular materials

In 60 BC Diodorus Siculus reports a golden honeycomb manufactured by Daedalus via lost wax casting. Then, the first honeycomb sandwich panel with skins pressed in a plastic incorporate into the core cell walls founded in 1937 by Claude Dornier [35].

The mechanical properties of honeycombs relied on cell geometry, the material's properties (Young's modulus, yield stress, fracture stress, and the relative density). The direction of the load applied [35]. When the aluminum honeycomb sandwich was made with non-flammable material, it stayed non-flammable [3].

The honeycomb core metallurgy process is a developing type of ultra-light engineering

materials. Porous metals are used for other essential purposes like light structures, energy management, vibration control, electromagnetic shielding, arresting flames, and catalytic engineering.

In general, a wide range of porous metal and cell structures can be used in aerospace, electronics and communication, transportation, atomic energy, medical, and environmental protection. Additionally, another modern technology applies to metallurgy, machinery, construction, electrochemistry, petrochemical, and bioengineering industries [3].

Besides the aluminum honeycomb structure, other cellular materials exist in nature. These materials have repeating internal geometry with inconsistent faces or edges. Just as materials have different pore size geometry, Aluminum honeycomb sandwich exists in other pore size structures. Example of cellular structure materials found in nature is shown in Figure 2.1.

2.2 Aluminum Honeycomb Sandwich Manufacturing

The honeycomb structure core is manufactured with a natural hexagonal shape. Mostly, honeycomb is produced in three ways: expansion, corrugation, and molding. Mainly, aluminum honeycomb is made by an expansion. The steps of the production of aluminum by expansion are:

- First, large thin sheets of aluminum are printed with discontinuous, parallel, thin strips of adhesive.
- Then, the sheets are stacked in a heated press while the adhesive bends.
- Next, the stake is sliced base on the desired thickness.
- Finally, the slice block gently stretched and expended to form the sheet of hexagonal cell shapes [33].

During curving aluminum, honeycomb does not require excessive mechanical force or heating [3]. Honeycomb can be manufacture with flat and curved shapes. The shape of the honeycomb cell is selected base on the engineering applications. The section of the honeycomb is

manufactured with regular hexagonal, triangular, square, circular-cored hexagonal, and circular-cored square [3].

Honeycomb sandwich panel assembled in two ways:

(1) Adhesive bonding technique: the method consists of using supplementary material to join skins and core. The advantage is that the structure of the component is not affected while joining. The disadvantage is that the process of bounding takes time and labor-intensive, and causes additionally weak skin to the core bond. Also, the technic can be applied with different methods such as thermoset and thermoplastic.

(2) Fusion bonding technique: the method consists of using a molecule exchange across the interface by fusion bonding of the skins and core. The advantages of fusion bonding manufacturing can be performed in short cycle times. Also, the fusion bunding technique applied with different methods such as vacuum molding, compression molding, and double-belt laminating make use of heat to soften the polymers and pressure to fusion bond the core and skins. The disadvantage is that the process of bounding takes two or more types of polymers. Therefore, the imbalance quantity of the polymers can affect the mechanical properties such as the sandwich's strength.

Jonas Grünewald et al. (2015) studied the manufacturing of thermoplastic composite (TPC) sandwich structures by fusion bounding technic. The result showed that:

- The fusion bonding utilizing vacuum molding, compression molding, or in situ foaming shows excellent potential for joining sandwich skins and core.
- The application of TPC skins and thermoplastic core materials for sandwich structures is advantageous due to material properties, minimized production cycle times, and environmental sustainability reasons.

The fusion bonding method offers an adhesive-free process, joining thermoplastic honeycomb core and face sheets during the production of the Aluminum honeycomb sandwich panel. Primarily, the

temperature must be precisely controlled during the process to guarantee the product quality. Therefore, a study was performed by:

Fan Xinvua et al. (2009) presented a mathematical model of heat transmission to analyze the transient temperature distribution from heating tools to the inner part of the core under fusion bonding conditions. It discovered that:

- The measured temperature results match the predicted ones during the heating stage. The model keeps valid results at the cooling stage, particularly at the center of gravity, the honeycomb.
- This model can be used for a wide range of honeycomb and face sheet materials if they can be fusion bonded in the double-belt laminator.

2.3 Aluminum Honeycomb Sandwich application

Aluminum honeycomb sandwich used for (energy absorption, filtration, sound reduction, magnetic protection, vibration damping, rigidness, lightweight panels, thermal insulation barriers, storage media, moisture resistance, and weight-saving esthetic, eco-friendly material, and heat exchanges). “Also, it might play a role in an impact-absorbing material in contact with heavy loads (e.g., polymer foams in a bicycle helmet)” [3].

Aluminum honeycomb sandwich materials can be transformed into diverse functional geometrical forms and deliver substantial performance advantages for weight-sensitive applications. Being strong and lightweight makes honeycomb an ideal material for the manufacture of crash helmets for racing car drivers, motorcyclists, and even bicyclists—the honeycomb is used as a weight-saving component than other materials with identical volumes. For the honeycomb's quality modeling (sound insulation), the cells can be filled with rigid foam for [3].

However, the low cost of manufacturing aluminum honeycomb sandwiches had extended the use of the material. According to Sadeep Sasidharan et al. (2019), a small amount of aluminum is required to produce honeycomb compare to dense products. Its high strength, weight-saving,

and minimum cost made Scientists and Engineers develop the usage of honeycomb sandwich with multiple industries (construction, sports equipment, automotive, etc.).

The main applications of aluminum honeycomb sandwich and porous metals are listed below:

- Closed variety is used for structural applications requiring load-bearing features and weight-saving and impact-absorbing structures like vehicle components.
- A wide variety is ideal for vibration and sound absorption and catalysis at high temperatures, such as heat exchange.
- Honeycomb sandwich can eliminate the opening and unwanted airflow of any structure.
- A wide variety is also useful in functional applications like vibration damping.
- Honeycomb sandwich with high strengths can act as high-capacity impact-energy absorbers.
- Honeycomb sandwich reduces the number of parts in the car frame, facilitates assembly, reduces costs, and improves performance in the aerospace, automotive industry [3].

Industry application of aluminum honeycomb sandwich are:

- In the construction field, aluminum honeycomb sandwiches are used as ceilings (subway stations, large shopping malls, conference rooms), curtain walls, roofs (high-rise buildings), screen dividers, soundproof panels, portable mobile homes (banks and hotels). Aluminum honeycomb sandwich can reduce the casualties and property losses caused by the earthquake.
- In aviation, ships, high-speed vehicles, aluminum honeycomb panels widely used in aviation, aerospace, transportation, construction military and other areas (rocket fairings, aircraft wings, and warehouses), train (bulkheads and floors), car (skins and doors), ceilings and curtain walls for building. In the application of wings and vertical tail, the cockpit, cargo floor, and the

door partition or cargo compartment. The honeycomb panels can effectively reduce aircraft weight and improve the handling sensitivity of moving parts [3].

2.4 Advantages of Aluminum Honeycomb Sandwich in Cold-Formed Steel (CFS)

The manufacturing of the aluminum honeycomb cold-formed steel (CFS) could optimize metal production and reduce waste. Aluminum honeycomb sandwich CFS material is obtained through a specific manufacturing process that usually occurs at room temperature, and there are many uses for aluminum honeycomb sandwich CFS—Figure II.2.

Figure 2.2 illustrates the penalization of aluminum foam CFS in construction.

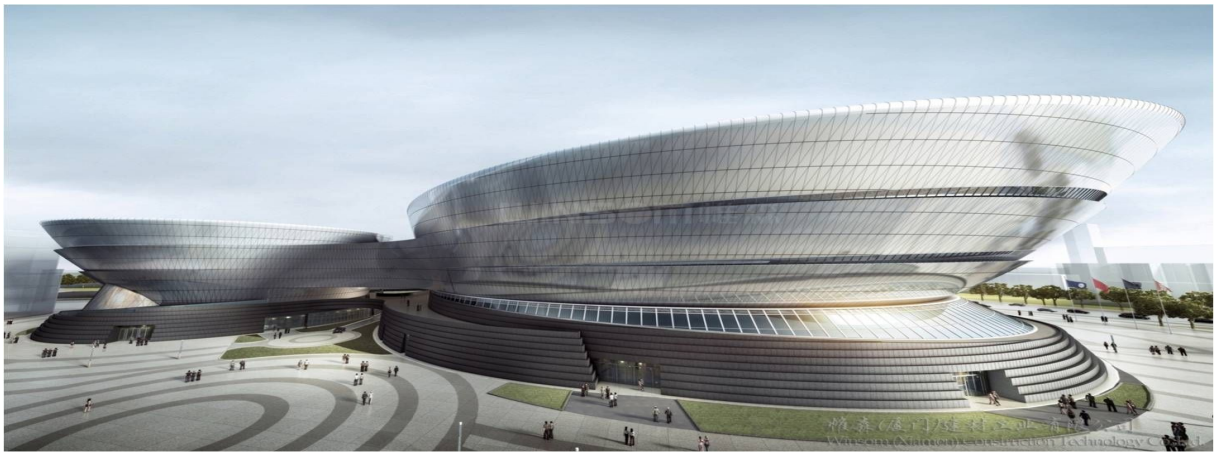

Figure 2.2: Aluminum panel for buildings

"Some advantages of cold-rolled steel allowed the aluminum foam to have the properties of fast modeling, high production, better coating, and massive plastic deformation of the metal. Selecting the right material for the project might significantly reduce costs while maintaining (or even improving) work quality and production" [14].

However, the high use of aluminum honeycomb sandwich for magnificent and sensitive structure required the modern manufacturing method to maintain the quality of the structure's fusion bound. "Therefore, adding-cold-foamed steel (CFS) framing systems during the production of aluminum honeycomb sandwich is beneficial in multiple ways such as:

- High strength-to-weight ratio relatively light
- Reduced construction waste
- Shorter project cycles
- Better results during wintertime
- Early project completion and budget savings
- Lower insurance rates and fire-related legal costs
- Product durability [10].

Mostly, cold-formed steel (CFS) framing has proven to be cost-effective, along with having sustainable benefits for mid-rise buildings and competitive building materials. "Cold-formed steel (CFS) framing has a proven track record of providing valuable and lasting benefits for mid-rise buildings and offers significant cost benefits over competitive" [16]. According to P.S. Liu et al. (2014), "In general, excellent corrosion resistance is essential for all structural attack" [15]. Additionally, "amorphous alloy has great propriety in resistance to be wear, abrasive, and corrosive, more specific strength and better energy absorption more than conventional porous metal" [4].

"Manufacturing aluminum honeycomb sandwich CFS has many advantages such as better cost, durability, sustainability, non-combustibility and resiliency, and ease of installation. In the future, there could be a better promise of the development of aluminum foam CFS" [2].

Importantly, aluminum can endlessly be recycled without losing its quality. Therefore, this makes it one of the most environmentally friendly metals on the planet. Incredibly, most of the aluminum ever produced is still being used today. G.P. Thomas (2014) confirmed that aluminum foams offer many benefits, such as:

- Very high specific stiffness and strength ratio

- Tremendous crush energy absorption capability
- Shock wave attenuation
- Vibration damping
- Thermal and sound insulation

Elsevier Ltd (2017) studied the crush behavior and the energy absorption capability of an aluminum honeycomb core in Abaqus, and mechanical test resulted from:

- Increases of the cell-wall thickness and the aluminum alloy's yield stress give higher crush loads and increase energy.
- Increases in cell size can decrease the energy-absorption capacity.

2.5 Finite Element Analysis

FEA is an engineering design tool used to evaluate many design prototypes for testing them in many different types of stresses (e.g., thermal, mechanical, etc.) before developing a prototype. There are many advantages and disadvantages associated with using FEA, and they are covered below.

FEA defines comprehensive result sets and generates a physical response of the system at any location, even neglected in an analytical approach. Safe simulation of potentially dangerous, destructive, or impractical load conditions and failure modes.

Multiple scholars used FEA and FEM (dentistry, biomedical engineering, civil engineering, mechanical engineering, etc.) to solve some unsolved problems related to their domain.

The use of FEA with engineering design allows humans to solve previously unsolved problems. Some of the advantages are:

- FEA can reduce the number of physical prototypes and optimize the final designs during the design phase to develop better and faster products.

- The solution to the design problem solved by FEA can be better visualized and understood at the very early stage of the design process ((such as a honeycomb sandwich with multiple layers), which allows designs to be corrected before manufacturing.

- FEA works by creating a complex geometry into a mesh network and elements of simpler equations called a mesh.

- FEA simulations can be observed through meshing for heat effects, stress effects, vibration effects, etc.

- FEA saves time and cost of the material during the modeling.

- It optimizes the honeycomb during the modeling (cutting, performance) by stimulating the sample's fracture and failure.

- FEA can illustrate the behavior (such as crack initiation and propagation) of the material by analyzing the result from a field and history output request.

According to Padmanabhan Krishnan (2015), FEA can handle complex:

- Geometry

- Analysis types

    - Vibration

    - Transients

    - Nonlinear

    - Heat transfer

    - Fluid

- Loadings

    - Node-base (points load)

    - Element-base (pressure, thermal, inertial forces)

    - Time-frequency

- Restrains analysis

- Indeterminate structures

Padmanabhan Krishnan (2015) stated FEA is limited to handle:

- Numerical problem
    - Computers only carry a finite number of significant digits
    - Round off and error accumulation
    - Can help the situation but not attaching stiff (small) elements to flexion (considerable) parts.
- Modeling errors with the user
    - Poor choice of element types.
    - Distort element
    - Inadequate geometric model
- Effect not automatic
    - Buckling
    - Large defections and rotations
    - Other nonlinearities

Study of the FEA application, advantages, and results tests are mentioned below by some scholars.

Sadeep Sasidharan et al. (2019) modeled and simulated a 20kW 8/6 SRM by using JMAG with FEA and the results validated with the theoretical design approach. They concluded:

- Increase the air gap's length, with a circular window on the rotor pole, smoothened the transition between rotor and stator by providing stator pole shoes and filleting the rotor-stator.
- Optimize geometry reduced the torque ripple by 100%.

Yongyu Ye et al. (2017) used the FE simulation to predict the effects of miniature channel-shaped across-the-thickness and across-the-width scratches that are difficult to manufacture. The study revealed that:

- The presence of both miniature channel-shaped across-the-thickness and width changed the fracture behavior of the wires in terms of the location of fracture initiation, the sequence of fracture propagation, and across-the-thickness scratch; neither acted as a crack initiator.

- Results serve as a tool for the fracture behavior and failure analysis for typical wires used for civil engineering applications containing miniature channel-shaped scratches that are not detectable by the present inline electromagnetic defect detection system. However, the effects on the fracture behavior of the wires were difficult to investigate experimentally.

S. Duczek et al. (2019) investigated an established mass lumping scheme. Several dynamic benchmarks are selected, showing that only suboptimal rates of convergence are attained if serendipity FE based on a diagonal mass matrix is employed.

J. M. P. Martins et al. (2016) performed an FEA of thermal contact by contact pressure and gap dimension in the heat flow across the two bodies' interface. They proposed a new law to define the interfacial heat transfer coefficient (IHTC) as a function of the contact pressure and gap distance, allowing a smooth transition between two contact status (gap and contact).

Catherine Amodeo et al. (2017) investigated two models I and II for pre-existing cracks of gas metal arc welds in lap-shear specimens. They instituted:

- The normalized computational stress intensity factor solutions for the idealized weld geometry matched the analytical solutions well.

- The FEA results can be used to estimate the fatigue lives and crack growth model under mixed-mode loading conditions for gas metal arc welds with unequal sheet thicknesses.

Aldemon L. Bonifácio et al. (2019) developed and compared two techniques to predict the mechanical properties of Lightweight Aggregate Concrete (LWAC). The FEM technique is applied to reproduce computationally through a 2-phase model, laboratory tests. In summary:

- Both FEM and SVR were technically feasible to estimate the compressive strength and modulus of elasticity of LWAC with minor deviations.

- Experimental procedures require significant time, cost, and materials to contribute to a safe, economical, and sustainable design of concrete mixtures.

M. Sesha Reddy et al. (2019) addressed the basics of FEA in dental implantology. They designed 3-D FEM to examine the implant, tooth, periodontal ligament, and bone. As a result clinicians can use this modern technology to enhance implant survival by well accepting the biomechanics of dental implantology

Tao He et al. (2018) reported computational cell-based smoothed FEM for fluid dynamics in incompressible flows and fluid-structure interaction (FSI). The main findings were summarized:

- SPGP technique is crucial to the second-order S-CBS scheme in incompressible flows and FSI. The stabilization parameter impacted numerical accuracy and efficiency.
- FSI solver never requires an accelerated fixed-point iteration, even a low mass ratio.

K.K Adewole et al. (2015) presented FE failure predictions and analyses of wire for civil engineering applications with various crack-like lamination types (Single and double), geometries (straight-end and inclined-end), and orientations (longitudinal, lateral, and transverse). The result illustrated that:

- FE failure analysis can be used for fractographic failure analysis.
- Fracture initiations do not always begin at the termini of every crack-like lamination; initiation only starts at the termini of inclined-end crack-like laminations.

Houman Zahedmanesh et al. (2012) investigated the growth of VSMCs in vascular scarf-folds with FEA and captured the critical characteristics of VSMC growth in TEBVs. They concluded that the model provided the valuable result of the mechanobiological processes that drive the remodeling process and regulate VSMC growth dynamics in TEBVs and elucidated mechanical factors' role (scaffold compliance and loading regime in this context).

Mohamed Shehata Aly (2007) compared the compressive stress-strain plots of the aluminum foams by the density and temperature changes. He concluded:

- The buckling of cell walls upon loading was the most deformation mechanism.

- Failure of cell walls took place due to cracks that propagated throughout the cell walls and caused the fracture.

Ryo Matsumoto1 et al. (2018) formed an FSPIF skin layer by pressing the powder and the cell wall of the foam in the IH process and stirred in the FSIF process. The skin layer at a maximum thickness of 1.4 mm is formed by a rotation rate of 8000 rpm, a tool feed rate of 60 mm/min, and 10 mm depth. They concluded that combination of sandwich structure and increase of bulk density, the specific plateau -a strain of the foam specimen with the skin layers improved up to approximately 1.2–1.6 times greater.

Abaqus CAE is used to visualize the results of the finite element analysis. Originally, Abaqus Company was founded in 1978 by Dr. David Hibbitt, Dr. Bengt Karlsson, and Dr. Paul Sorensen with the original name Hibbitt, Karlsson & Sorensen, Inc., (HKS). “Later, the company name was changed to ABAQUS Inc. before the acquisition by Dassault Systems in 2005” [7].

The product is popular with academic and research institutions in engineering. The software can intensify modeling. Also, the program can customize the material. Furthermore, the design of an element in Abaqus could illustrate the physical behavior of the material in a wide range of modeling.

Every complete finite-element analysis has five separate stages: for a list, refer to Figure 2.3.

Figure 2.3: Five stages of completing finite element analysis

CHAPTER 3

THESIS STATEMENT

The thesis objective is to analyze, model and test an aluminum honeycomb sandwich structure in 4 steps:

(1) Three actual aluminum honeycomb sandwich samples were obtained from the UNT Department of Materials and Science Department.

(2) FEA analysis (in ABAQUS) shall be performed on three simulated Aluminum Honeycomb sandwich Structures that mimic the samples.

(3) Aluminum honeycomb sandwich shall Mechanical tested on the three pieces with each compressive test, and two samples with the bending test along with mechanical testing on the simulated ABAQUS models.

(4) The sample behavior will be analyzed for compression vertical, compression horizontal, and shear wall through multiple loadings.

The objective is to determine how the sandwich's physical characteristics impact the sandwich's mechanical properties. Determine under what conditions the specimens will be lighter and mechanically stronger.

CHAPTER 4

RESEARCH METHODOLOGY

The methodology compares experimental testing and Abaqus stimulation of aluminum honeycomb sandwich provided by the UNT Department of Material Science and Engineering through a research collaboration agreement. Three different tests (vertical compression tests, horizontal compression tests, and bending tests) determine the honeycomb sandwich specimen's mechanical properties.

Additional mechanical properties are defined, including the poison's ratio, young modulus, elastic stress-strain, modulus of resilience, ultimate stress-strain, fracture stress-strain, modulus toughness, engineering stress, engineering strain, true stress-strain, shear forces, bending moment, maximum deflection, and displacement.

4.1 Mechanical Properties of Aluminum

Aluminum is a perfect metal in several ways. It has a high resistance to heat and corrosion, high electrical conductivity, lightweight properties, and chemical stability.

According to P.S. Liu (2014), aluminum is easy to recycle, floats effortlessly in water, and can be very fire-resistant. Aluminum can be curved, cut, and welded to any desired shape, so modern architects cannot create buildings that would be impossible to make from wood, plastic, or steel [35]. Aluminum can melt at 650 °C, cast, formed, and machined, and conduct electric current.

Here some of the mechanical properties of aluminum:

- Light way: aluminum is a very lightweight material with a specific weight of 2.7g/cm^3, about a third of the steel.
- Corrosive resistance: aluminum naturally produces a thin oxide coating. It is useful for material exposed to a corroding environment.

- Ductile: Aluminum processed in different ways (such as sheets, foil, tubes, wires, geometrical configuration, etc.)
- Very high specific stiffness and strength ratio.
- Impermeable and odorless: Even aluminum foil at 0.007mm thickness.
- Non-magnetic and nontoxic: aluminum is adequate electric shielding (computer disk, magnet housings). And nontoxic (used for cooking utensils)
- Non- sparking aluminum produces no sparks if in contact with non-ferrous metal or its self.
- Recyclable: aluminum is a hundred percent recycle. It makes it the most cost-effective source material.
- Tremendous crush energy absorption capability: aluminum is an excellent sound and energy absorbent (use for construction ceiling)
- Vibration damping.
- Thermal and sound insulation. [17] and [34].

According to Jaroslav et al. (2018), the mechanical properties of the aluminum honeycomb is illustrated in Table IV.1.1.

Table 4.1: The mechanical properties of the aluminum honeycomb

Properties mechanic	Unit	Value
Density	lb./in³	0.03937
Young modulus	Ksi	10,500
Poisson ratio	-	0.33
Temperature of melt	˚c	650

4.2 Engineering Stress-Strain

Because the sample is made of aluminum, the aluminum properties mechanic is used to model and analyze the Abaqus simulation. Therefore, the true stress-strain is evaluated and resulted in Abaqus's data for the plasticity properties (yield. stress, and strain).

Engineering strain is defined as the amount of deformation in the applied force direction divided by the initial material length. It was expressed by Eq. 2.1:

$$\varepsilon=\Delta L/L \qquad \text{(Eq. 2.1.)}$$

Engineering stress is defined as the load divided into the initial cross-section area of the sample. The engineering stress is shown by Eq. 2.2:

$$\sigma e=P/Ai \qquad \text{(Eq. 2.2)}$$

where: σe = engineering stress, P= pressure, Ai= cross-sectional area of the specimen, ε= strain, ΔL= variation of the length, and L= original length.

Mostly, the strain is the response of a material to applied stress. When the component is loaded with a force, it produces stress, causing the material to deform.

The parameters defined as below:

According to Esther A. et al. l (2012), aluminum engineering stress and strain are illustrated in Table 4.2.

Table 4.2: Engineering stress-strain of the aluminum

Strain (in/in)	Stress (Ksi)
0	0
0.003714	39
0.01172	44.5
0.02052	48
0.03131	50.5
0.04047	52
0.06199	54.5
0.07985	56
0.107985	57.5
0.15427	60

4.3 True Stress-Strain

True strain is defined as a natural log of one and the engineering strain. The true strain is illustrated by Eq. 2.3:

$$\varepsilon t=\ln(1+\varepsilon) \quad \text{(Eq. 2.3)}$$

True stress isd the the load divided by the sample's cross-section area at that instance and is a true indicated internal pressure. The true stress is defined by Eq. 2.4:

$$\sigma= \sigma e^* (1+\varepsilon) \quad \text{(Eq. 2.4)}$$

where εt= true strain, ε= engineering strain, and σe = engineering stress.

The true stress and strain of the aluminum honeycomb sandwich result utilized as a properties mechanic during the sample simulation. The final result of the true stress-strain is illustrated in Table 4.3.

Table 4.3: True stress-strain of the aluminum

True Strain (in/in)	True Stress (Ksi)
0	0
0.00370712	39.144846
0.011651853	45.02154
0.020312301	48.98496
0.030829839	52.081155
0.039672534	54.10444
0.060144507	57.878455
0.076822143	60.4716
0.10254305	63.7091375
0.14346811	69.2562

True stress and strain define plastic behavior (such as aluminum) by considering the actual dimensions. The aluminum honeycomb sandwich plots include elastic and plastic zone. Therefore,

it is logical to use true aluminum stress and strain data during the Abaqus honeycomb sandwich analysis.

Elasticity is the deformation of a solid material that reverses its original condition once the external load is removed.

However, plasticity is a non-reversible deformation of the solid material. Here, once the external load is removed, some deformation remains.

The true stress-strain and the engineering stress-strain plots of the aluminum revealed the same tendency. Also, the two plots were identical from the elastic region. However, the aluminum's true stress-strain plot was higher than the aluminum's engineering stress-strain at the plastic area. This difference originated by integrating the strain over the entire test.

Finally, the aluminum honeycomb sandwich has both a plastic and elastic property base on the stress applied to the honeycomb sandwich. The result of the engineering stress-strain and the true stress-strain plotted to illustrate the aluminum's final behavior. For illustration, refer to Figure 4.1.

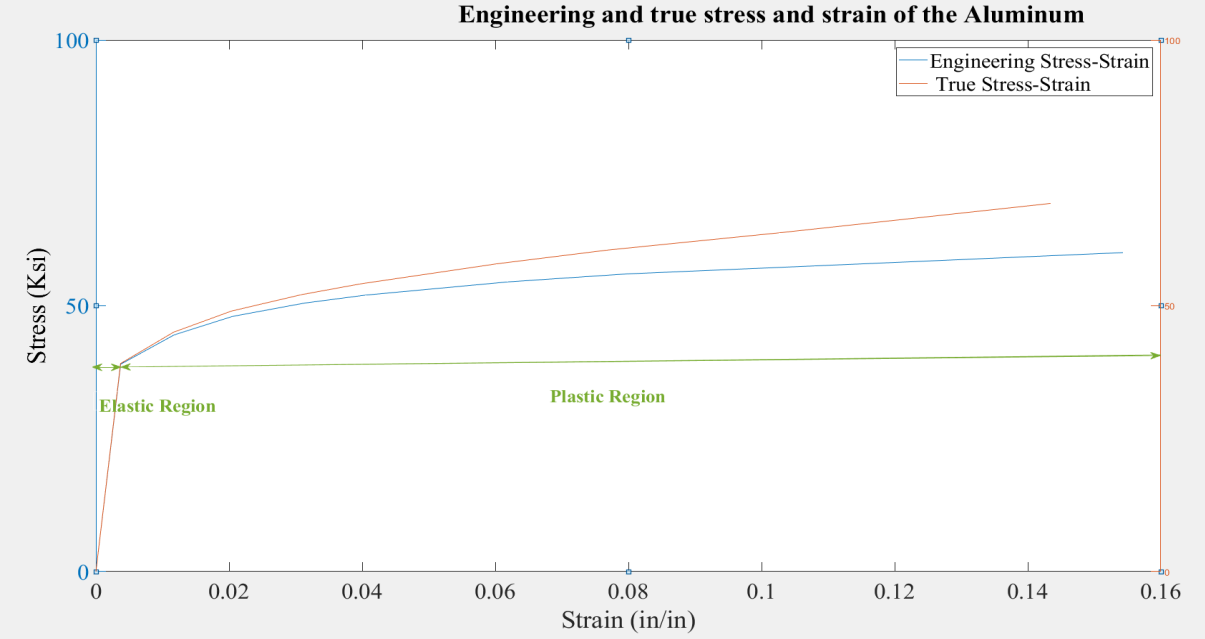

Figure 4.1: Comparison of the plots between the engineering stress-strain and true stress strain

4.4 Compressive Test

Three sample aluminum honeycomb sandwiches (Sample 1, S2, and S3) were compressed to evaluate the aluminum honeycomb sandwich mechanical properties. The displacement test will be delivered by UNT (Discovery Lab F162) INTRON-4482C4859 testing machine. The standard compression test will be ISO/DIS 13314 E (compression test for porous and cellular metals with 50 % or more porosity. This test will be carried out at room temperature and under quasi-static rate conditions).

This compressive test measures the honeycomb compressive stress-strain (elasticity, ultimate, fracture). The modulus of resilience, modulus of toughness, modulus of elasticity, and the occupancy calculated modulus of resilience, toughness. Also, determine the stress-strain (elasticity, ultimate, fracture), density, young's modulus, poison's ratio.

The dimensions of compressive vertical and horizontal for the sample are identical. The compressive vertical is represented by the samples Sample 1, S2, and S3. The compressive horizontal is represented by S4, #5, and S6.

Aluminum is a perfect metal in several ways. It has a high resistance to heat and corrosion, high electrical conductivity, lightweight properties. Each sample was made of aluminum and assembled with three layers: the top layer, the bottom layer, and the honeycomb layer inserted between two thin panels of aluminum (top and bottom layers) for illustration refer to Figure 4.2 and Table 4.4.

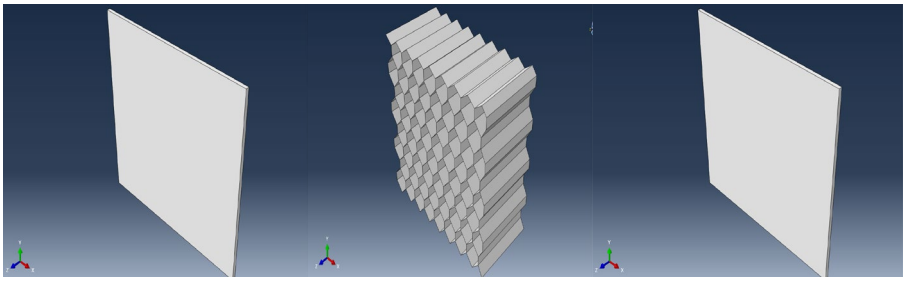

Figure 4.2: Honeycomb sandwich

Table 4.4: Honeycomb sandwich layers dimensions in compression

Parameter (Unit)	Top Layer	Honeycomb Layer	Bottom Layer	Honeycomb Shell	Tolerance of Error
Length (in)	2	2	2	-	± 2%
Weight (in)	2	2	2	-	± 2%
Thickness (in)	0.03937	1	0.03937	0.003937	± 2%

4.5 Compression Vertical of Aluminum Honeycomb Sandwich Set-Up

4.5.1 Mechanical Test

A compressive vertical was performed on the honeycomb sandwich. Therefore, a pressure load was applied to the sample vertically at the top layer. Figure 4.3 illustrates the mechanical test set up of the compressive vertical.

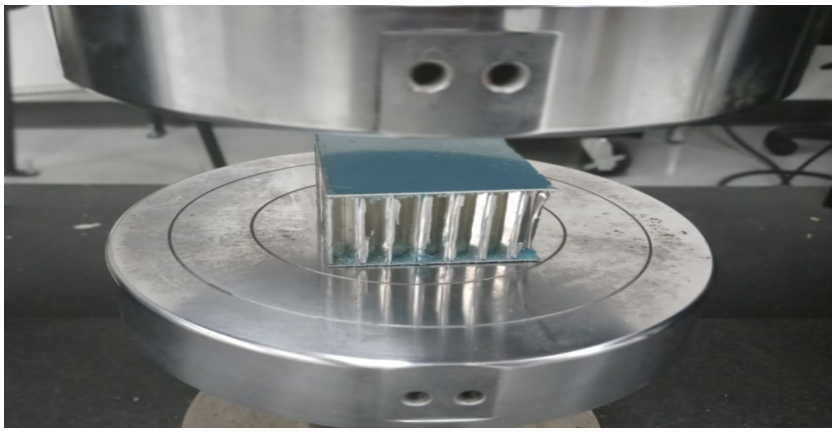

Figure 4.3: Compression vertical testing set-up of INSTRON-4482C4859 machine

4.5.2 Abaqus Simulation

A compressive vertical simulated on the honeycomb sandwich. Therefore, a pressure load was applied to the sample vertically at the top layer. The boundary condition used encapsulated. The seeding adopted for each part was 0.01 inches.

The result of the simulation was collected at the center of the top layer with Node 452. The gravitational node was chosen because it is essential to understand the stability of the honeycomb

sandwich. If the part is subjected to an unbalanced force in some areas, the forces rotate at the region's gravity. Also, it is the point where the uniform pressure of the part acts. It makes it easier to solve some mechanical problems with a complicated element, such as a honeycomb sandwich.

Also, a pressure load is applied vertically to the top layer of the sandwich. The pressure loads' setup with the compressive vertical in Abaqus is illustrated in Figure 4.4.

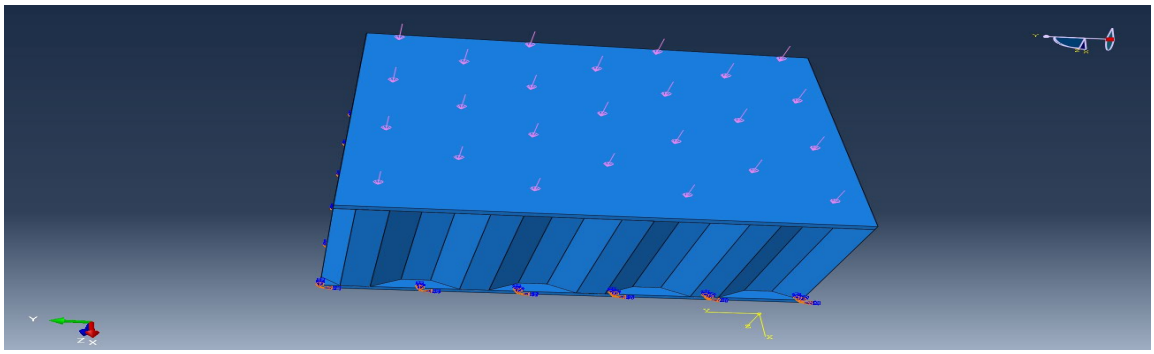

Figure 4.4: Compressive vertical of the honeycomb sandwich loaded at the top layer

4.6 Compression Horizontal of Aluminum Honeycomb Sandwich Set-Up

4.6.1 Mechanical Test

A compressive Horizontal was performed on the honeycomb sandwich. Therefore, the pressure load was applied to the sample horizontally at the sandwich base on the thickness (top, honeycomb, and bottom layer). The testing setup for the compression horizontal is illustrated in Figure 4.5.

Figure 4.5: Compression horizontal testing set-up of INSTRON-4482C4859 machine

4.6.2 Abaqus Simulation

The aluminum honeycomb sandwich was compressed Horizontally with Abaqus. Therefore, a pressure load was applied to the sample horizontally at a surface depth (top, honeycomb, and bottom layer). The boundary condition used encapsulated. The seeding of each part was adopted at 0.01 inches.

The simulation result was collected at the honeycomb layer with Node 1151. A pressure load is applied horizontally to the sandwich (at a surface depth) of the sandwich. The testing setup for the compression horizontal in Abaqus is illustrated in Figure 4.6.

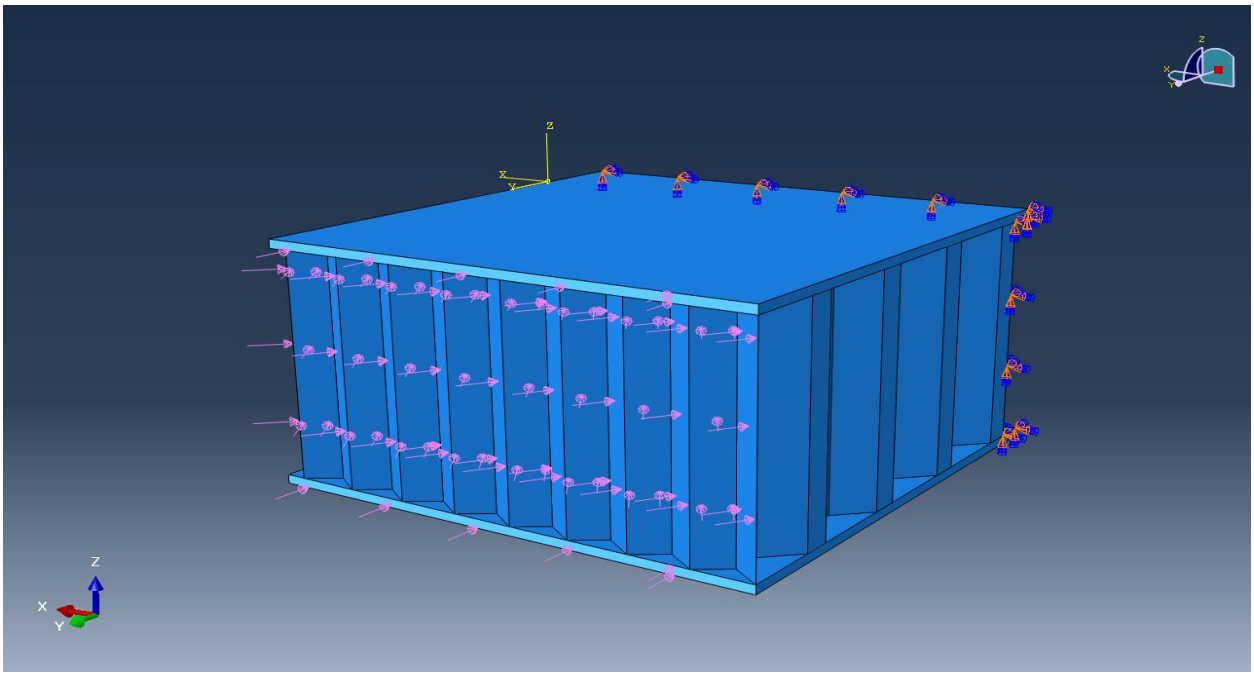

Figure 4.6: Compressive horizontal of the honeycomb sandwich loading

4.7 Bending Test

Two aluminum honeycomb sandwich specimens (Bend 1 and Bend 2) were tested to evaluate FEA mechanical properties. The displacement test shall be performed by a UNT Discovery lab SHIMADZU AGS-X machine using the three-point bend test. The standard used is

ASTM E 290 (Bend test for flat metal material. Assigned for three points bend test at either 90-degrees or 180-degree angle).

This test was carried out at room temperature and under quasi-static rate conditions. This bend test measures the sandwich's maximum displacement completed at 1inch, and maximum bending stress, strain, and forces.

Two aluminum honeycomb sandwichs (Bend 1 and Bend 2) were tested mechanically and simulated in Abaqus. Each part was made of aluminum and assembled with three layers: the top layer, the bottom layer, and the honeycomb layer inserted between two thin panels of aluminum (top and bottom layers) for illustration refer to Figure4.7 and Table 4.5.

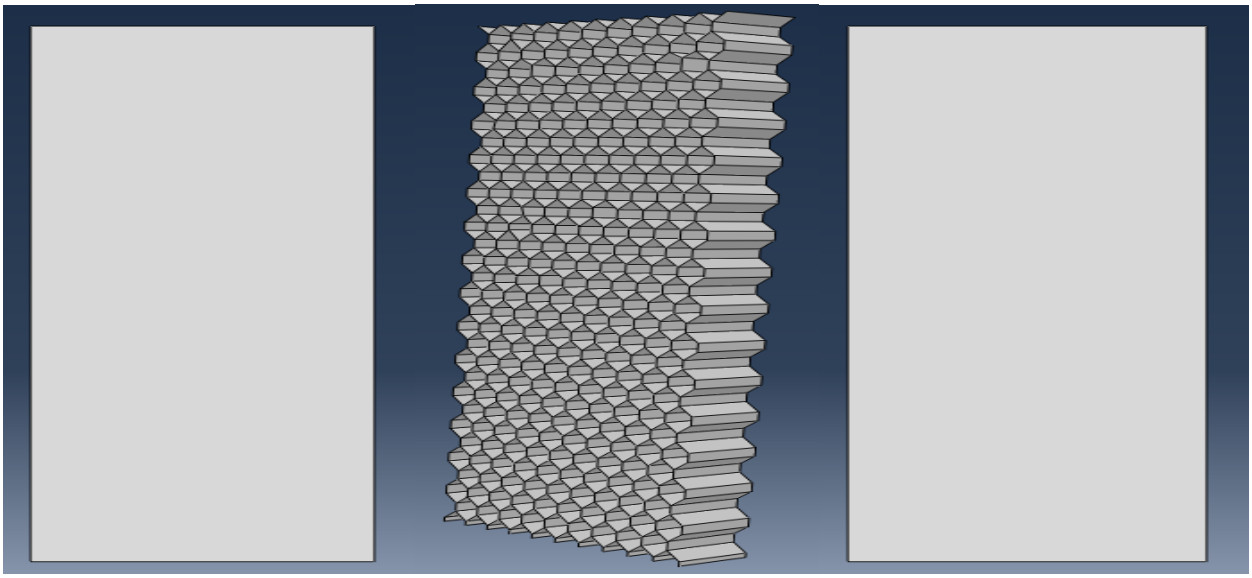

Figure 4.7: Honeycomb layers

Table 4.5: Honeycomb sandwich layers dimensions in bending test

Parameter (Unit)	Top Layer	Honeycomb Layer	Bottom Layer	Honeycomb Shell	Tolerance of Error
Length (in)	11.90	11.90	11.90	-	± 2%
Weight (in)	4	4	4	-	± 2%
Thickness (in)	0.03937	1	0.039370	0.00393701	± 2%

4.7.1 Mechanical Test of Aluminum Honeycomb Sandwich 3-Point Bend Set-Up

A three points bend performed on the honeycomb sandwich linear pressure load was applied to the mid-section of the sample vertically at the top layer. Figure 4.8 illustrates the mechanical test set up of the bending test.

Figure 4.8: Test fixture on test resource machine for the three-point bend

4.7.2 Abaqus Simulation of Aluminum Honeycomb Sandwich 3-Point Bend Set-Up

A tree points bend simulated on the honeycomb sandwich in Abaqus. Therefore, a linear pressure load was applied to the sample vertically at the mid-section top layer. The boundary condition used was the displacement rotation. The seeding of each part was adopted at 0.2 inches.

The simulation result was collected at the centerline of the top layer with a set of 20 nodes (node number 600; 608; 637; 644; 655; 662; 673; 680; 691; 698; 1304; 1305; 4415; 4418; 4419; 4422; 4428; 4429; 4430 and 4431). A linear loading defined the sample's total energy because it was the most stressed part of the sample, and the displacement was 1 inch.

The three points bend setup in Abaqus is illustrated in Figure 4.9.

The aluminum honeycomb structure is material when stressed, behave both as an elastic or plastic material. The test result shows the aluminum honeycomb stress, ultimate strain point, and fracture point during the research.

The energy absorbed was calculated from each sample by defining the modulus of resilience and the toughness. However, no apparent yield point was detected for the test data (mechanical and the gravitational Node 452) plotted in compression vertical. The modulus resilience and the modulus of toughness results illustrate the sandwich's behavior, such as brittle or ductile material. Definition and characteristic of each term shown below.

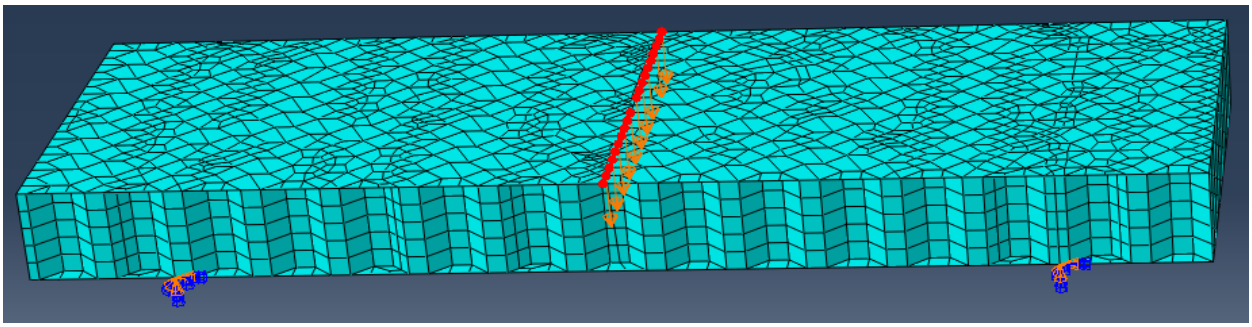

Figure 4.9: Three points bend set in Abaqus

4.7.3 Compressive Vertical Displacement

The honeycomb sandwich compressive vertical test from both simulation and experimental test illustrated that:

- ·The collapses began from the section of the honeycomb shells. Originated from the honeycomb hexagonal hallow shell-wall, a high volume of the pores, and the fusion bound.
- The top layer and the bottom layer both preserved their shape after the test—the high density of aluminum produced from both layers.
- Honeycomb sandwich demonstrated a moving crack propagation from both experimental and simulation test results at the honeycomb's mid-section. However, the propagation crack was linear along to the honeycomb layer. It was instigated by the shell thickness and the presence of the hexagonal hollow cell.

CHAPTER 5

EXPECTED RESEARCH RESULTS

This research intends to use FEA by studying aluminum honeycomb sandwich behavior in Abacus and through mechanical tests.

5.1 Compression Test

The aluminum honeycomb structure is material when stressed, behave both as an elastic or plastic material. The test result shows the aluminum honeycomb stress, ultimate strain point, and fracture point during the research.

The energy absorbed was identified from each sample by defining the modulus of elasticity, resilience, and toughness. However, the four plots did not have an exact yield point for the compression vertical. The modulus resilience and the modulus of toughness results illustrate the sandwich's behavior, such as brittle or ductile material. Definition and characteristic of each term shown below:

The modulus of resilience is the material's ability to absorb energy when stressed in the elastic region. The goal of defining the modulus of resilience is to detect the range of energy a material can absorb to ovoid plastic deformation. Also, it can illustrate the maximum energy absorbed per unit volume without creating a permanent distortion.

The stress-strain plot was integrated from zero to the elastic limit to found the sandwich's modulus of resilience. Also, we can use the method of two points average to define the area. The unit of the modulus elasticity is in kilo pound by square inch (Ksi). During the process, we can define the elastic modulus, strain, and stress.

The elastic modulus is the slope of the yield point of the elastic stress and strain. It is founded on the linear equation of the modulus resilience.

Modulus of toughness is the ability of the material to absorb energy before fracture. Also, the modulus of toughness shows the absorbed energy in plastic deformation.

The ultimate stress is the highest value of compressive stress. The goal to outline the maximum strength an element can hold before failure.

Base on the result, the material can behave as a ductal or brutal material. Here some of the compressive test behavior and characteristic:

Ductal is the ability of a material to deform plastically before fracturing. Some of the measures of ductility are elongation and area. Mostly ductile material has:

- A large plastic region
- A considerable compression strains
- Reduce localize strain
- High toughness

Mostly brutal material has:

- A low plastic deformation
- Low or even no yield strain
- The compressive strain is less than 5%
- Low modulus of toughness
- Considerable strain concentrated on the fracture crack tips

5.1.1 Compressive Vertical Displacement

The honeycomb sandwich compressive vertical test from both simulation and experimental test illustrated that:

- The collapses began from the section of the honeycomb shells. Originated from the honeycomb hexagonal hallow shell-wall, a high volume of the pores, and the fusion bound.

- The top layer and the bottom layer both preserved their shape after the test—the high density of aluminum produced from both layers.

- Honeycomb sandwich demonstrated a concentric crack propagation from both experimental and simulation test results at the honeycomb's mid-section. However, the propagation crack was linear along to the honeycomb layer. It was instigated by the shell thickness and the presence of the hexagonal hollow cell.

For illustration, refer to Figures 5.1 and 5.2.

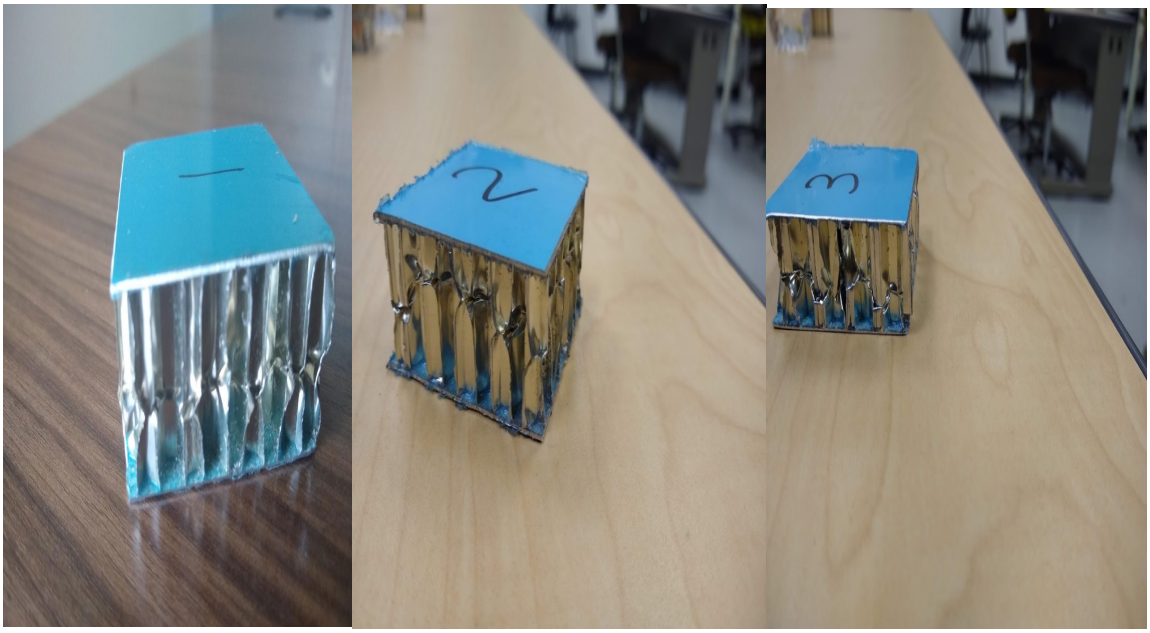

Figure 5.1: Compression vertical of S1, S2, and S3

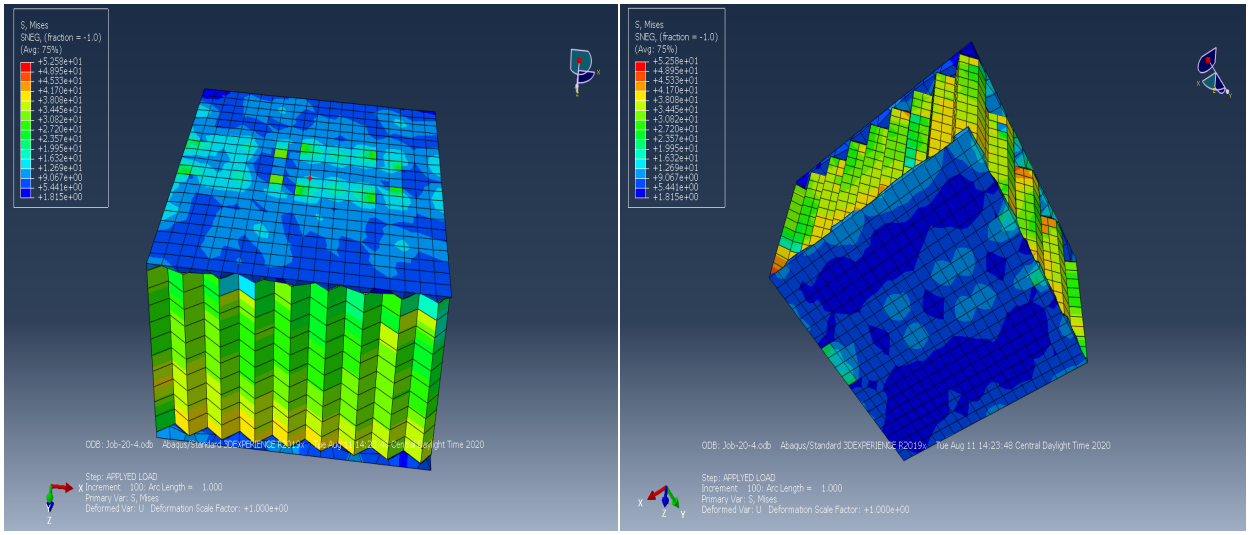

a-Top layer view b- Bottom layer view

Figure 5.2: Compressive vertical simulation of the honeycomb

The honeycomb sandwich compressive vertical plots shown that the discrepancy between the simulated and experimental deformation patterns increased as the strain increased (See Figure 5.3). The compressive strengths of the aluminum founded from the simulation were higher than those of the experiment.

The discrepancy of the hexagonal cell walls, the thickness, the density of the material, and the fusion bonding has affected the test result.

As the strain increased for the compressive vertical, the stress gradually increased, and local fracture of the cell wall began to occur immediately after the compressive stress reached its maximum value. After crack initiation, the vertical compressive stress gradually decreased with increasing compressive strain owing to crack propagation by the continuous fracture of the hexagonal shell wall, then the final fracture occurred. The aluminum honeycomb exhibited brutal behavior due to the ductile nature of the pure Al base material.

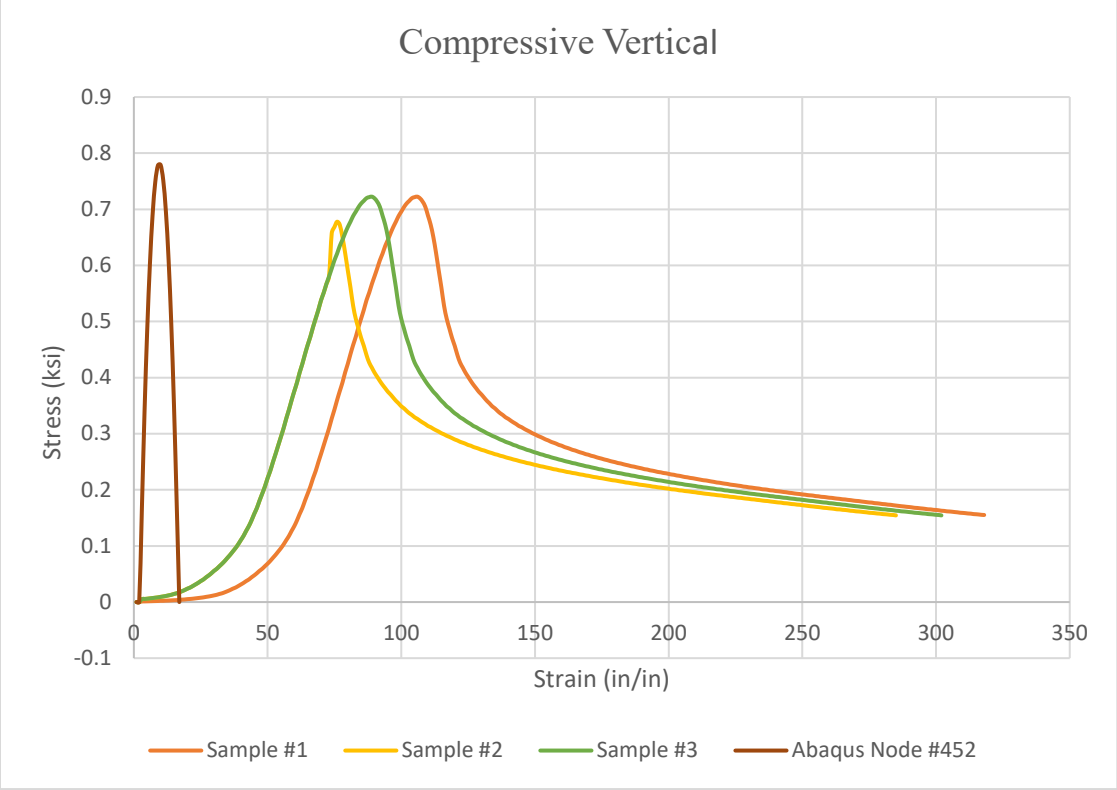

Figure 5.3: Plots with Abaqus and mechanical tests with compression vertical

The four plots illustrated a similar tendency. However, the simulation on the Abaqus of gravity of the top layer was more significant than the mechanical test. The differences between real and predicted pore cells wall affected the sandwich's compressive vertical results—the disparity of the hexagonal distribution of the honeycomb's cell wall, the density of each layer.

Both test (Abaqus and mechanical) images with compressive vertical shows where the crack is initiated and propagated (honeycomb shell layer). The damage was linear in the midsection of the honeycomb layer. Therefore, the sandwich demonstrated a moving crack propagation from both experimental and simulation test results.

Abaqus simulation of an aluminum honeycomb sandwich provided a suitable result. With the field output request and the history output request, the sandwich's behavior was defined at the top layer's gravity. The node assigned was number 452 (refer to Figure.1.2). The magnitude of the simulation was 4 Ksi. The meshing technique seems appropriate for modeling FEA, such as an aluminum honeycomb sandwich (such as modeling, viewing, optimizing, etc.).

5.1.2 Properties Mechanic of the Honeycomb Sandwich with Compression Vertical

5.1.2.1 The Modulus of Elasticity and Modulus of Resilience

5.1.2.1.1 The Modulus Resilience of Sample 1

S1 elastic region is plotted by Figure 5.4.

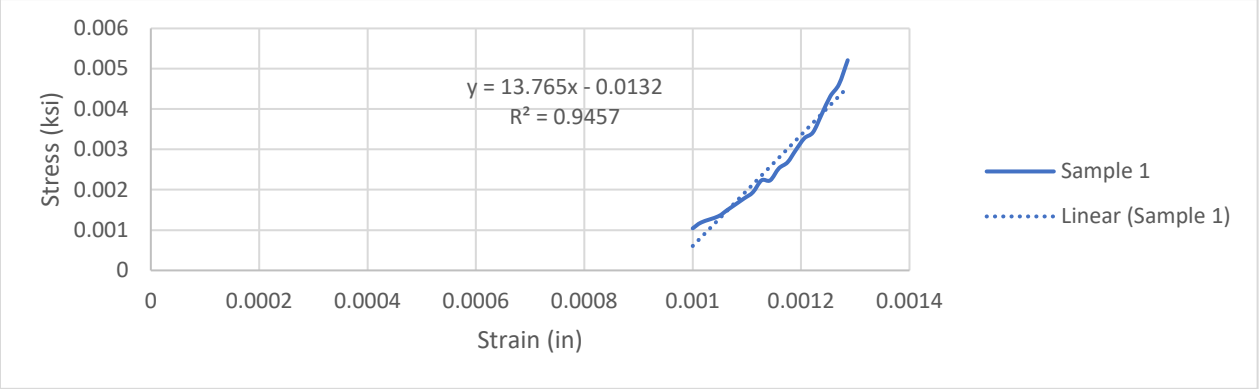

Figure 5.4: Modulus resilience of Sample 1

The formula the modulus of elasticity of Sample 1 is the linear Eq. 5.1, which is equal to 13.76Ksi. At the elastic strain and stress, respectively, 0.001286 % and 0.005521 Ksi. With an accuracy of 94.57% from Eq. 5.2.

$$y = 13.765x - 0.0132 \quad \text{(Eq. 5.1)}$$

$$R^2 = 0.9457 \quad \text{(Eq. 5.2)}$$

The modulus resilience of Sample1 is the energy absorbed by the elastic region solved by integrating the linear Eq. 5.1 at the strain value from 0 - 0.001286:

$$\int_0^{0.001286} Y(x)$$

$$\int_0^{0.001286} [(3.765x - 0.0132)d(x)$$

$$Y(x)=\left[\frac{x*(68825*x - 132)}{10000}\right]_0^{0.001286}$$

The modulus of resilience of Sample 1 is 1.3861929×10−5 ksi.

The same procedure is done with the S2, S3, and Node 452

5.1.2.1.2 The Modulus Resilience of Sample 2

Elastic region of S2 is shown by Figure 5.5.

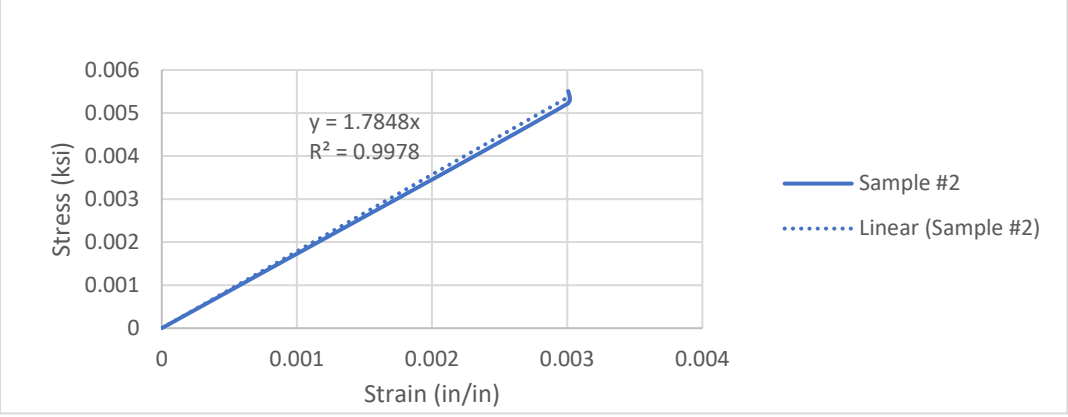

Figure 5.5: Modulus resilience of Sample 2

The modulus elasticity of Sample 2 is illustrated by the slope of the linear Eq. 5.3 which is equal to 1.7848Ksi. At the elastic strain and tress correspondingly 0.003 % and the elastic stress 0.005211 Ksi. With a precision of 99.78% from Eq. 5.4.

$$y = 1.7848*X \quad \text{(Eq. 5.3)}$$

$$R^2 = 0.9978 \quad \text{(Eq. 5.4)}$$

The modulus of resilience of Sample 2 is 8.06747943×10−6 Ksi.

5.1.2.1.3 The Modulus Resilience of Sample 3

The elastic region is illustrated by Figure 5.6.

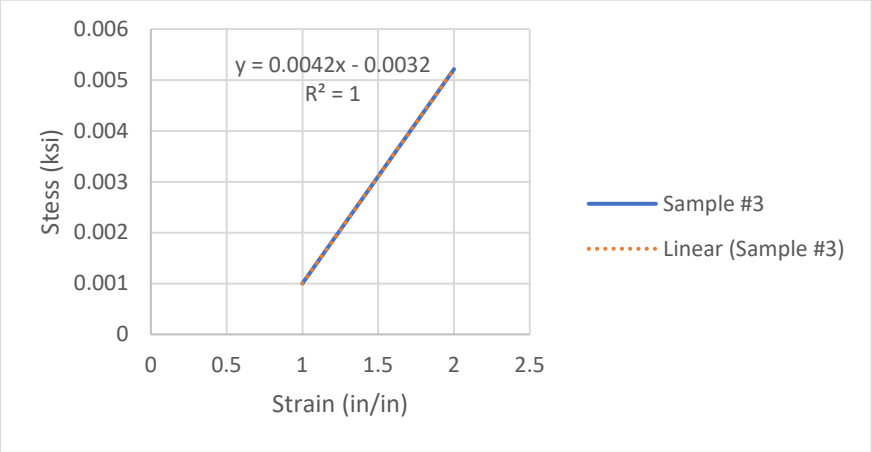

Figure 5.6: Modulus resilience of Sample 3

The modulus of elasticity of Sample 3 is the slope of the linear Eq. 5.5 which is equal to 0.0042. At the elastic strain and stress, respectively 0.0052% and 0.00511 Ksi. With correctness of 100% from Eq. 5.6.

$$y = 0.0042x - 0.0032 \quad \text{(Eq. 5.5)}$$

$$R^2 = 1 \quad \text{(Eq. 5.6)}$$

It was calculated by integrating Eq. 5.6 at the strain value from 0 to 0.005.

The modulus of resilience of Sample 3 is 1.66188599×10−5 Ksi.

5.1.2.1.4 Abaqus Simulation with Node 452

Simulation of the aluminum honeycomb sandwich elastic region is plotted by Figure 5.7.

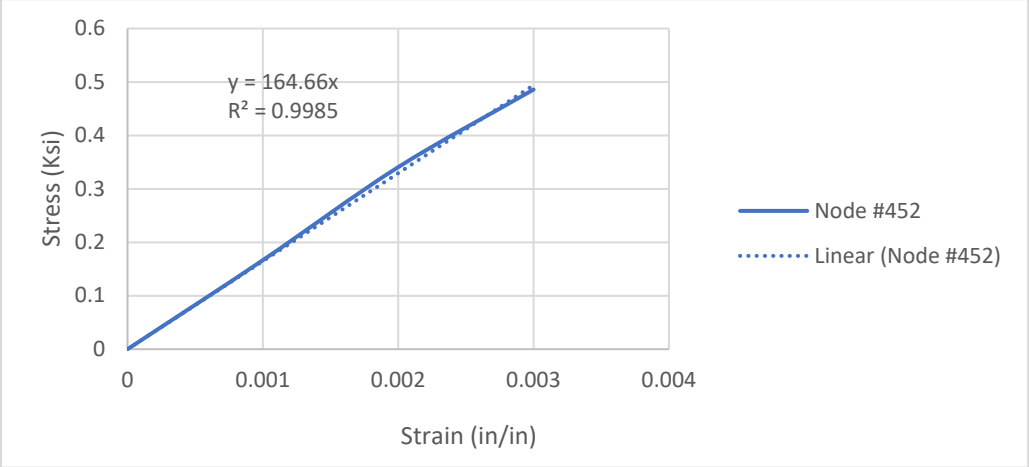

Figure 5.7: Abaqus simulation with Node 452 elastic modulus

Eq. 5.7 shows the modulus of elasticity, which is 164.66 Ksi. At the elastic strain and stress, respectively 0.006% and 0.04858 Ksi. With an accuracy of 99.85% from Eq. 5.8.

$$y = 164.66*X \quad \text{(Eq. 5.7)}$$

$$R^2 = 0.9985 \quad \text{(Eq. 5.8)}$$

The modulus of resilience of Node 452 was 3.3912×10−4 Ksi.

The data of modulus resilience of the aluminum honeycomb with the compression axial is illustrated in the Table 5.1.

Table 5.1: Modulus of elasticity and resilience with the compressive vertical

Test	Elastic Strain (in/in)	Elastic Stress (Ksi)	Modulus Elasticity (Ksi)	Modulus of Resilience (Ksi)	Confidence (%)
S1	0.001286	0.0055211	13.765	1.39E-05	94.57
S2	0.003006693	0.005211	1.7848	8.06747943×10−6	99.78
S3	0.005211215	0.00511	0.0042	1.66188599×10−5	100
Abaqus N452	0.003	0.4858	164.66	3.3912×10−4	99.85

Test	Elastic Strain (in/in)	Elastic Stress (Ksi)	Modulus Elasticity (Ksi)	Modulus of Resilience (Ksi)	Confidence (%)
Range	0.001286-0.005211215	0.00511 – 0.4858	0.0042-164.66	8 E-6 -3.39 E-4	94.57-100
Avg	0.003125977	0.125410525	45.0535	9.44E-05	98.55

The lowest and the highest elastic strain occurred respectively with the Sample 1 and S3, with an average elastic strain of 0.0031%. Also, S3 and Node 452 are shown, respectively, the lowest and the highest strength of the elastic region with an average value strain of 0.125. Abaqus simulation had the most modulus of elasticity. However, S3 had the bottommost modulus elasticity of the aluminum honeycomb compressive test.

With the elastic region, the simulation with Abaqus had the most modulus of reliance, and the S2 had the least energy absorption in the plastic region. The average of the modulus elasticity was about 9.44E-05. The overall of the study of the modulus resilience confidence was 98.55%

Table 5.2 illustrates the ultimate stress-strain of the mechanical test and Abaqus simulation with Node 452.

Table 5.2: Ultimate stress and strain with the compressive vertical

Test	Ultimate	
	Strain (in/in)	Stress (ksi)
Sample 1	0.002656	0.722465
Sample 2	0.00357	0.672434
Sample 3	0.001544489	0.719485655
Abaqus N3452	0.008	0.7791
Range	0.001544-0.008	0.6772434-0.7791
Average	0.003942622	0.723371164

The ultimate points data illustrate that S3 and Node 452 had the least and the high value of the compressive strain, respectively. However, the S2 and the Abaqus simulation successive had the lowest and the highest amount of the ultimate stress. With an increase of 13%of strength.

5.1.2.2 The Modulus of Toughness

According to S. McLeod (2019), the confidence for interval point is 95%, and as the sample size narrow the mean of the sample size become more accurate.

The modulus of the toughness of the elements was calculated by the method of average point by Eq. 5.9:

$$A=\frac{(X2-X1)*(Y2-Y1)}{2} \quad \text{(Eq. 5.9)}$$

where A is the modulus of toughness, X1 is the first strain, X2 is the final strain, Y1 is the first stress, Y2 is the final stress.

5.1.2.2.1 Sample 1 Modulus Toughness

The fracture point of Sample 1 was noticed at the strain 0.001286 % and the stress at a value 0.155154 Ksi. Figure 5.8 illustrates the energy absorbed in the plastic region of Sample 1.

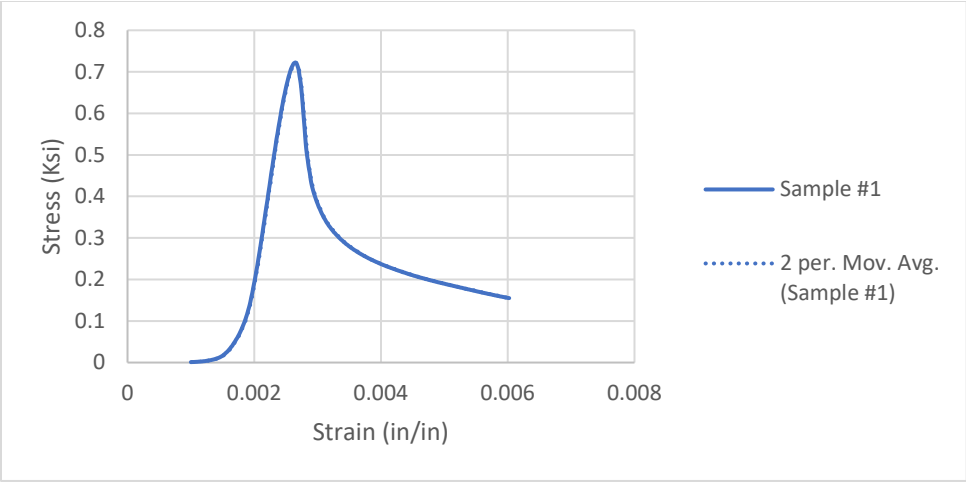

Figure 5.8: The modulus of toughness of Sample 1

The modulus of the toughness of Sample 1 was calculated using the average point method in Eq. 5.9. From the origin 0 throughout 0.006023 strain, and the stress from 0 to the0.155154 Ksi.

$$A=\frac{(0.006023-0)*(0.155154-0)}{2}$$

The modulus of the toughness of Sample 1 is 9.34492542 E-4 Ksi.

5.1.2.2.2 Sample 2 Modulus Toughness

Sample 2 noticed 0 0.0015386 % fracture strain and 0.67243387788 Ksi fracture strength. The energy absorbed at the plastic region of Figure 5.9 illustrates Sample 2.

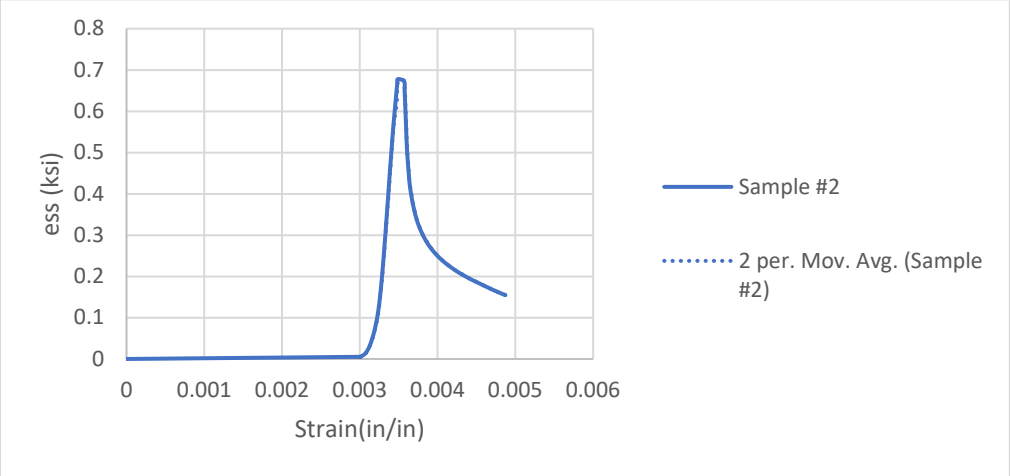

Figure 5.9: The modulus of toughness of Sample 2

The modulus of the toughness of Sample 2 was calculated by moving average by using Eq. 5.9. Therefore, at range 0 to 0.006023 strain, and from 0 thru 0.155154 Ksi strength.

$$A=\frac{(0.001538583508-0)*(0.67243387788-0)}{2}$$

The modulus of the toughness of Sample 2 is 5.17297837E-4 Ksi.

5.1.2.2.3 Sample 3 Modulus Toughness

The fracture points Sample 3 noticed at 0.00287% strain and 0.6724 Ksi strength. Figure 5.10 illustrates the energy absorbed in the plastic region of Sample 3.

The modulus of the element's toughness is calculated by moving the average point in Eq. 5.9. Therefore, the first strain was 0; the final strain was 0.006023; the first stress was 0, and the final stress was 0.155154 Ksi.

$$A=\frac{(0.002871655094-0)*(0.15441035556-0)}{2}$$

The modulus of the toughness of Sample 3 is 2.21706642E-4 Ksi.

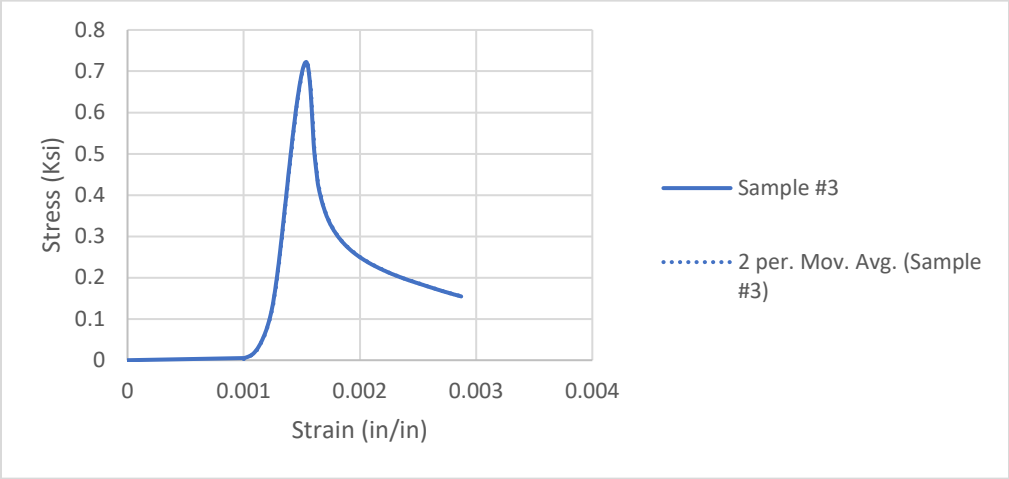

Figure 5.10: The modulus of toughness of Sample 3

5.1.2.2.4 Abaqus Simulation with Node 452 Modulus Toughness

The fracture point of Node 452 was noticed at the strain 0.00287% and the stress at a value 0.6724 Ksi. Figure 5.11 illustrates the energy absorbed at the plastic region with Abaqus simulation.

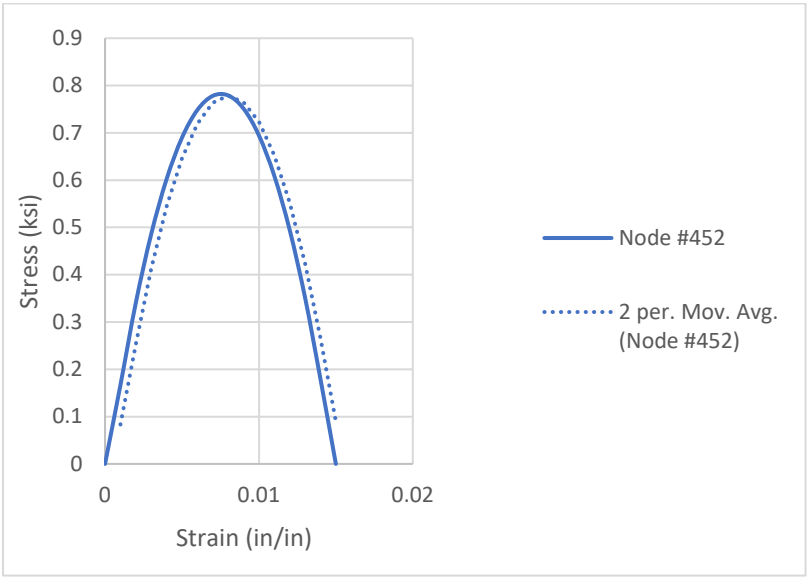

Figure 5.11: The modulus of toughness of the in Abaqus with Node 452

The modulus of toughness of the node was calculated by moving the average point in Eq. 5.9. The strain ranged from 0 to 0.006023, and the stress was from 0 to 155154 Ksi.

$$A=\frac{(0.012-0)*(-0.1793)}{2}$$

The modulus of the toughness of Node 452 was 10.758×10−4Ksi.

The modulus toughness of the compressive vertical is illustrated in the Table 5.3.

Table 5.3: Modulus of the toughness for the compressive vertical

Test	Fracture Strain (in/in)	Fracture Stress (Ksi)	Modulus of Toughness (ksi)	Confidence (%)
Sample 1	0.00602	0.15515	9.34492542 E−4	95
Sample 2	0.00154	0.67243	5.17297837 E−4	95
Sample 3	0.00287	0.15441	2.21706642 E−4	95
Abaqus N 452	0.014	0.1793	10.76 E-4	95
Range	0.001538584-0.014	0.154410356-0.1793	2.217 E-4 - 10.76 E-4	95
Average	0.00611	0.29032	6.87E-04	95

Based on test data, the fracture strain ranged from 0.0015 through 0.014 with the low and high values strain were noticed respectively with the S2 and Abaqus simulation with an average strain of 0.006%. Besides, the fracture strength showed a least and a high energy absorption data successively with the Sample 1 and Abaqus simulation. Moreover, the average strain was 0.29 Ksi.

The energy w absorbed at the plastic region with compressive vertical shows that Abaqus simulation had the most modulus toughness. However, the S3 had the least energy absorbed. The average modulus toughness of the test was 6.87E-04. The overall of the study of the modulus resilience confidence was 95%.

Based on the test result with the vertical compressive test, the aluminum honeycomb sandwich had:

- No yield point for the four actual test data plots.
- Low modulus elasticity ranging from 8 E-6 Ksi-3.39 E-4Ksi
- Low modulus toughness from 2.217E-4 Ksi to– 10.76E-4 Ksi.
- Low fracture strain from 0.001538584-0.14 below 5%
- A concentric crack propagation at the samples' midsection from both tests (mechanical test and Abaqus simulation).

In conclusion, the aluminum honeycomb sandwich behaved like a brutal material, with the compressive vertical.

5.2 Compressive Horizontal of the Aluminum Honeycomb Sandwich

The honeycomb sandwich compressive horizontal tests from both simulation and experimental test illustrated that:

- The collapses began from the horizontal surface of the honeycomb shells. The failure originated from the hexagonal hollow shell-wall, the density, and the fusion bound.
- The top and the bottom layer collapsed parallelly at the sample's depth (horizontal surface from the section).
- The three layers noticed a horizontal collapse of the sandwich.
- The damage was initiated by the inconsistency of the sandwich's density and the distribution of the fusion bond.
- Honeycomb sandwich demonstrated a concentric crack propagation from both experimental and simulation test results. However, the propagation crack was parallel at the stressed area of the sandwich. For illustration, refer to Figures 5.12 (mechanical test) and 5.13 (Abaqus simulation).

As the stress increased for the compressive horizontal, the strain gradually increased, and local fracture of the cell wall began to occur immediately after the compressive stress reached its maximum value. After crack initiation, the horizontal compressive stress gradually decreased with increasing compressive strain owing to concentric crack propagation by the continuous fracture of

the cell wall, then the final fracture occurred. The aluminum honeycomb exhibited brutal behavior of the aluminum.

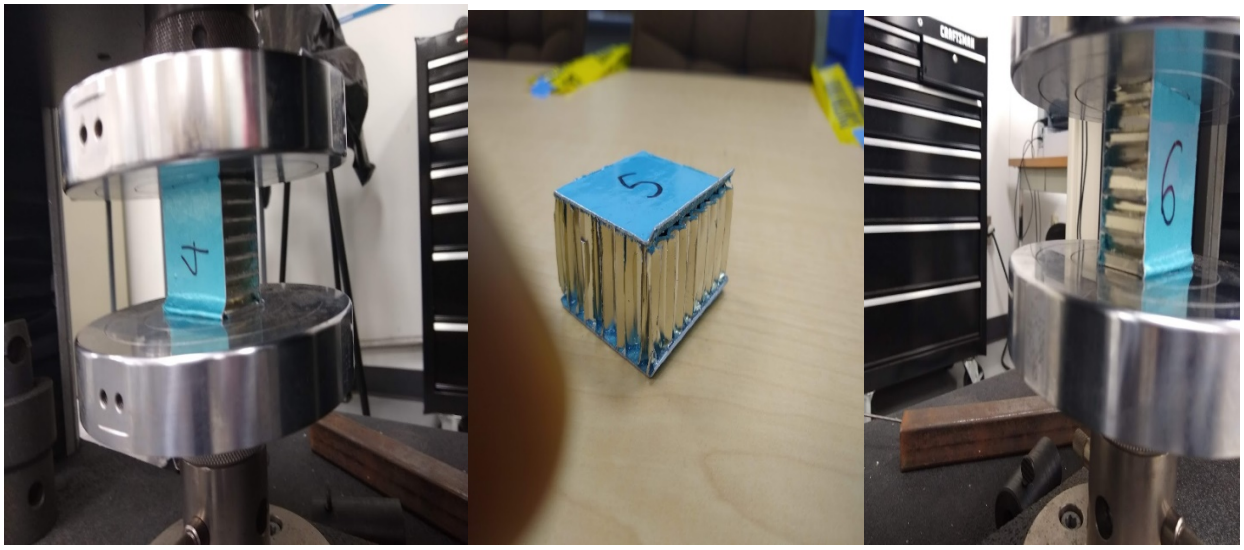

Figure 5.12: Compression horizontal of samples S4, S5 and S6

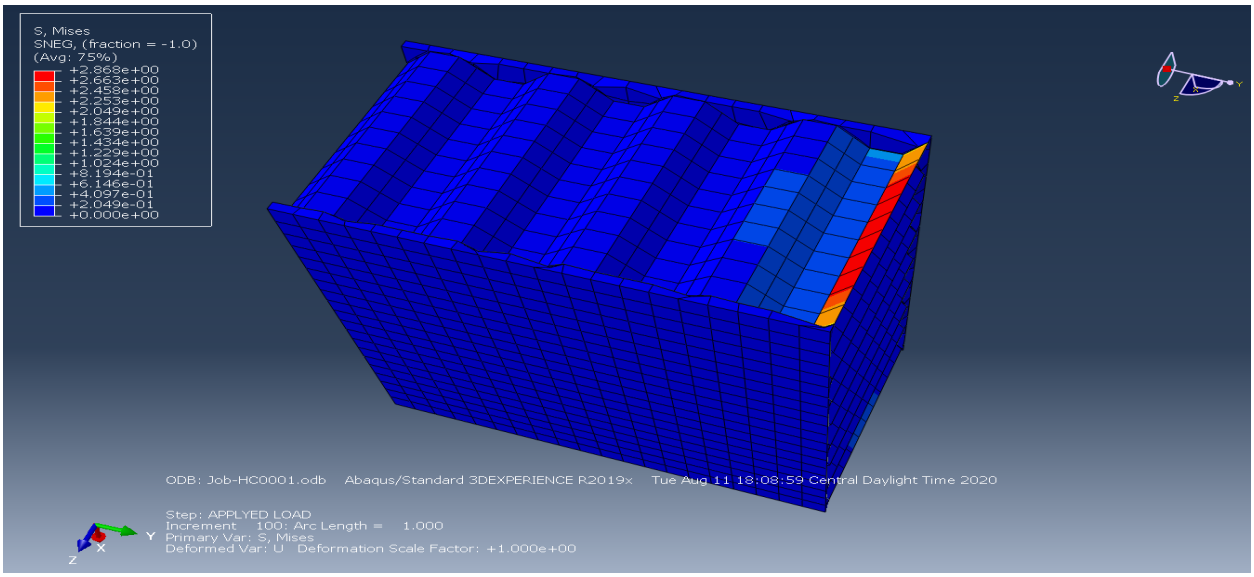

Figure 5.13: Compressive horizontal simulation of the honeycomb sandwich

Then the top layer and the bottom layer both collapsed parallelly at the horizontal base of the sample. Instigated by the increases of the strain, the stress rapidly increased, and fracture occurred immediately at the top and bottom layer of the section after the compression stress reached its maximum value. The honeycomb layer exhibited severe fracture, attributed to the

density and the sandwich layers' fusion bond.

Abaqus simulation with the compressive horizontal at the node number 1151 plot shown the highest compressive stress-strain plot. The differences between real and predicted pore cells wall affected the aluminum sandwich's compressive test results from the disparity of the hexagonal distribution of the honeycomb's cell wall. For illustration, refer to Figure 5.14.

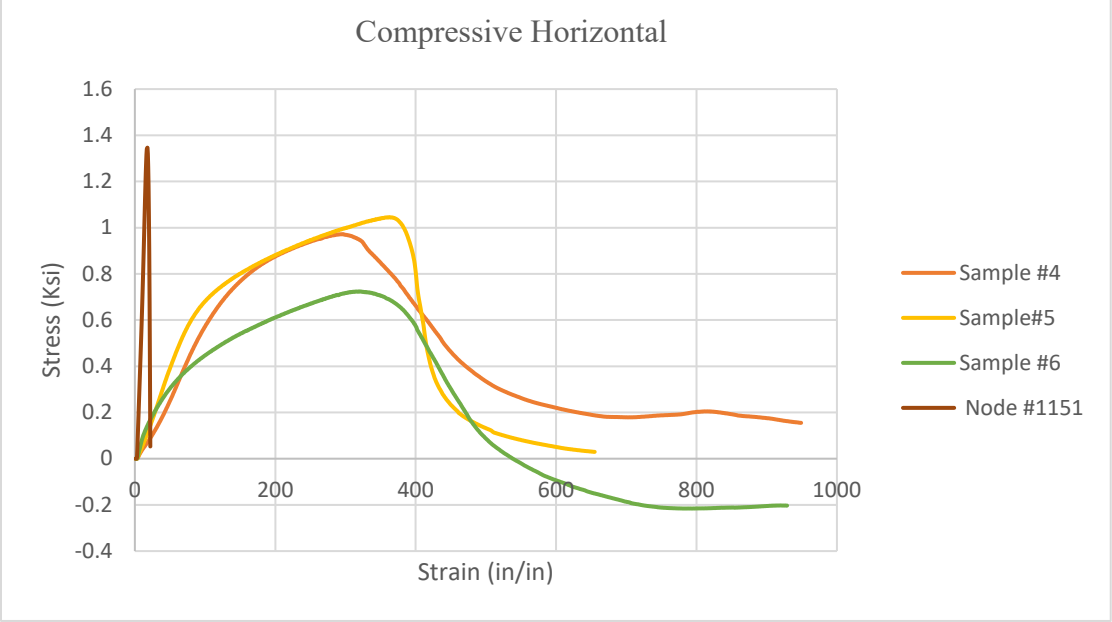

Figure 5.14: Plots with Abaqus and mechanical tests with compression horizontal

The four plots of the compressive horizontal had the same tendency. The four plots did not have an exact yield point. Therefore, the simulation of an aluminum honeycomb sandwich with Abaqus provided a suitable result. Based on the field output request and the history output request, the aluminum honeycomb sandwich's behavior was defined (compressive horizontal).

FEA in Abaqus with the honeycomb sandwich show where primarily the crack was initiated (honeycomb shell layer) and propagated (bottom and top layers) with a long-predefined interface such as bonded sheets of the honeycomb sandwich.

Honeycomb sandwich demonstrated a moving crack propagation from both experimental and simulation test results.

Abaqus simulation of an aluminum honeycomb sandwich shows an appropriate result. Based on the field output request and the history output request, the sandwich's behavior is apparent. The node selected was number 1151 (refer to FigureV.2.2). The magnitude of the simulation was 0.01 Ksi.

5.2.1 Properties Mechanic of the Aluminum Honeycomb Sandwich with Compression Horizontal

The compressive horizontal has not shown any yield point from the mechanical and simulation results.

5.2.1.1 The Modulus of Elasticity and Modulus of Resilience

5.2.1.1.1 The Modulus Resilience of Sample 4

The modulus resilience is the energy absorbed by the elastic region. Sample 4 modulus elasticity is plotted by the Figure 5.15.

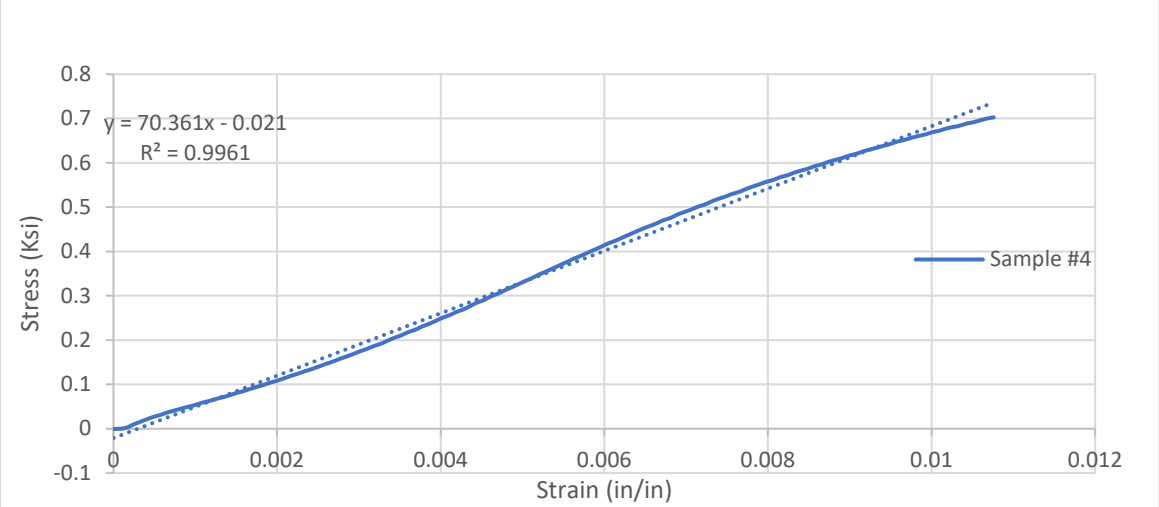

Figure 5.15: Modulus resilience of Sample 4

Based on the formula, the modulus of elasticity is the slope of the linear Eq. 5.10 which is equal to 70.361 Ksi. At the elastic strain and strength, respectively, 0.001286 % and 0.005521 Ksi. With an accuracy of 99.61% from Eq. 5.11.

$$y = 70.361*X - 0.021 \quad \text{(Eq. 5.10)}$$

$$R^2 = 0.9961 \quad \text{(Eq. 5.11)}$$

The modulus of resilience of Sample 4 was calculated by integrating Eq. 5.10 at the strain value from 0 - 0.001286 strain.

$$\int_0^{0.01076} Y(X)$$

$$\int_0^{0.01076} [(70.361 * X - 0.021)\mathrm{d}(x)$$

$$Y(x)=\left[\left(\frac{x*(70361*x-42)}{2000}\right)\right]_0^{0.01076}$$

The modulus of the resilience of Sample 4 is 0.003847153857 ksi**.**

The same procedure was done with the S5, S6, and Node 1151.

5.2.1.1.2 The Modulus Resilience of Sample 5

Figure 5.16 plots Sample 5 modulus elasticity.

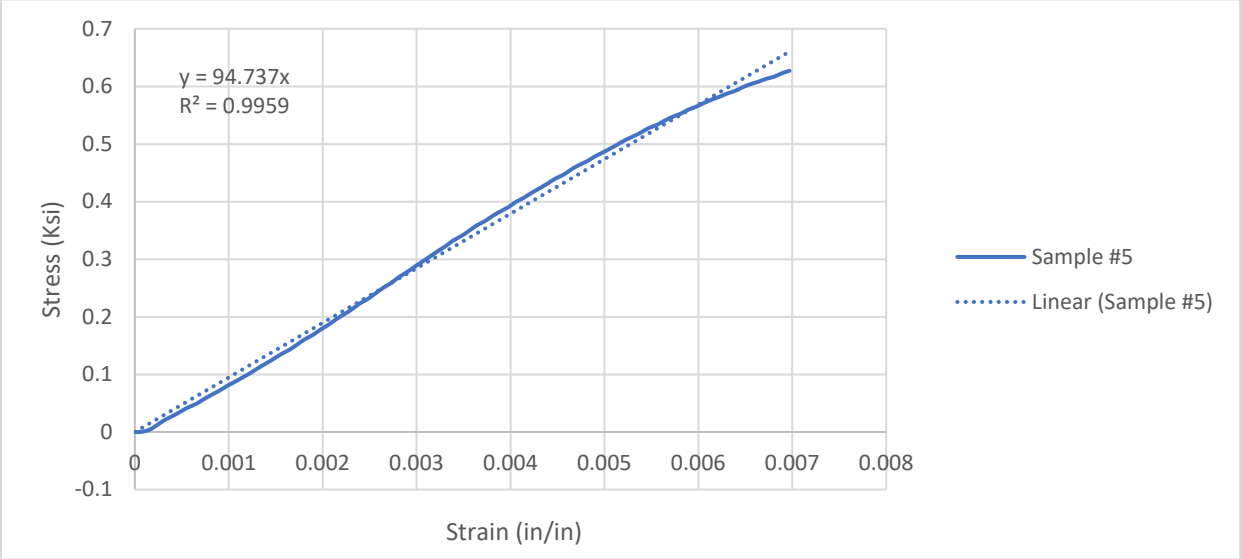

Figure 5.16: Modulus resilience of Sample 5

Base on the formula, the modulus of elasticity is the slope of the linear Eq. 5.12 which is equal to 94.737 Ksi. At the elastic strain and strength, respectively 0.00697% and 0.62708 Ksi. With an accuracy of 99.59 % from Eq. 5.13.

$$y = 94.737*X \quad \text{(Eq. 5.12)}$$

$$R^2 = 0.9959 \quad \text{(Eq. 5.13)}$$

The modulus of resilience of Sample 5 is defined by integrating Eq. 5.12 at the strain value from 0 - 0.00697 strain.

The modulus of the resilience of Sample 5 is 0.002301204362 **ksi.**

5.2.1.1.3 Modulus Resilience of Sample 6

Figure 5.17 plots Sample 6 modulus elasticity.

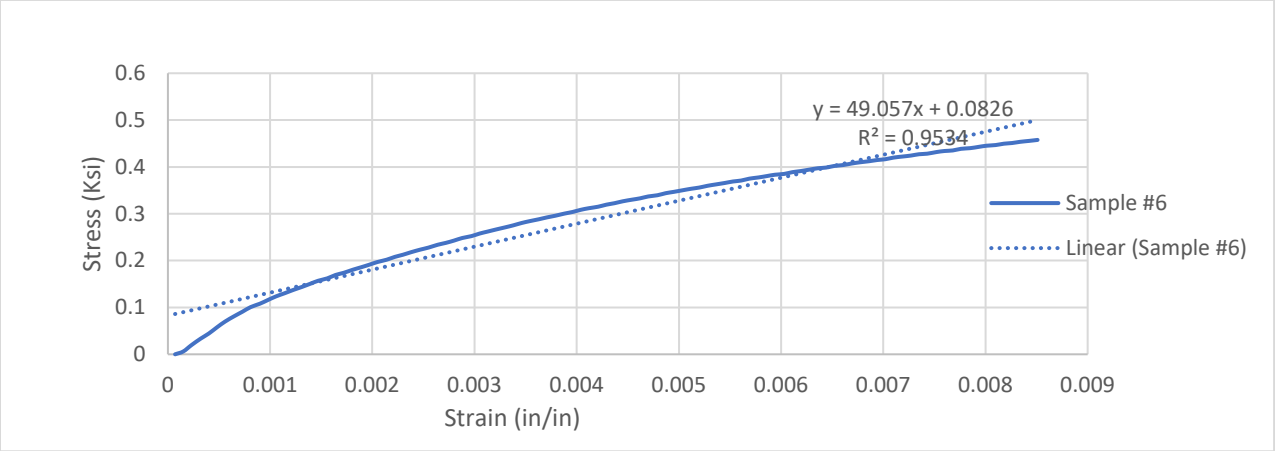

Figure 5.17: Modulus resilience of Sample 6

Based on the formula, the modulus of elasticity is the linear Eq. 5.14 which is equal to 49.057 Ksi. At the elastic strain of 0.00851% and the elastic stress 0.4576 Ksi. With an accuracy of 99.59 % from Eq. 5.15.

$$y = 49.057*X + 0.0826 \quad \text{(Eq. 5.14)}$$

$$R^2 = 0.9959 \quad \text{(Eq. 5.15)}$$

The modulus of resilience of Sample 5 is integrating Eq. 5.14 at the strain value from 0 - 00.00851 strain.

The modulus of the resilience of Sample 6 is 0.002479282423 Ksi.

5.2.1.1.4 Modulus Resilience in Abaqus with Node 1151

Figure 5.18 plots the node modulus elasticity

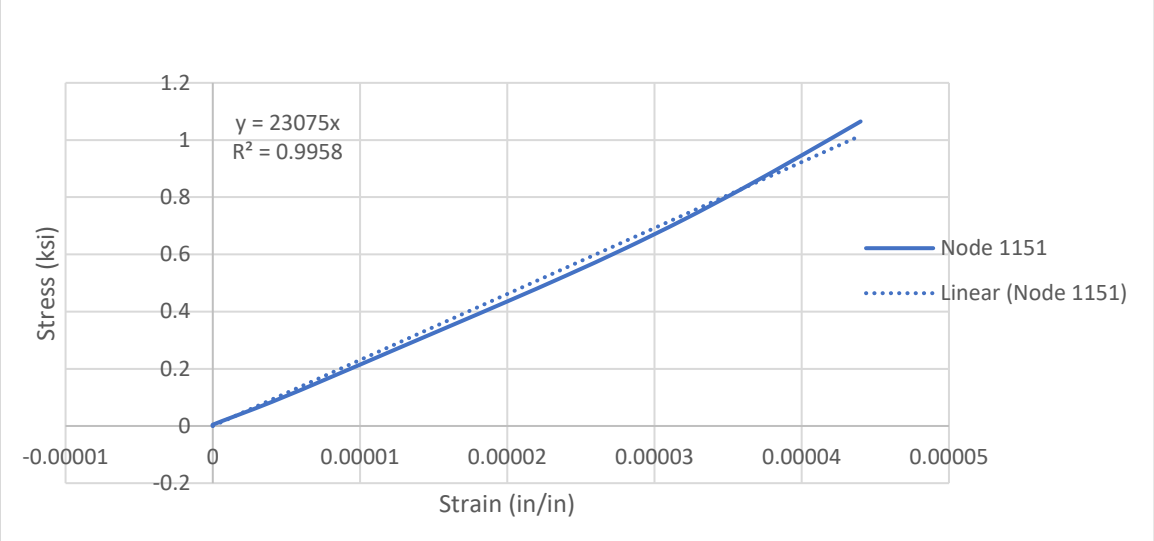

Figure 5.18: Modulus resilience of Node 1151

The modulus of elasticity is the linear Eq. 5.16, equal to 23075 Ksi. At the elastic strain of 0.000044% and the elastic stress of 1.065Ksi. With an accuracy of 99.59 % from Eq. 5.17

$$y = 23075*X \quad \text{(Eq. 5.16)}$$

$$R^2 = 0.9958 \quad \text{(Eq. 5.17)}$$

The modulus of resilience of the node is the integration of Eq. 5.16 at the strain value from 0 - 00.00851 strain.

The modulus of resilience of Node 1151 is 2.23366×10^{-5} Ksi**.**

The modulus resilience data of the aluminum honeycomb with the compression horizontal is illustrated in the Table 5.4.

Table 5.4: Modulus of elasticity and resilience with the compressive horizontal

Test	Elastic Strain (in/in)	Elastic Stress (Ksi)	Modulus Elasticity (Ksi)	Modulus of Resilience (ksi)	Confidence (%)
S4	0.01076	0.62708	70.361	0.00385	99.61
S5	0.00697	0.4576	94.737	0.0023	99.59
S6	0.0085	1.065	49.057	0.00248	95.34
Node 1151	4.4E-05	0.4576-1.065	23075	2.23E-05	99.58
Range	0.00004-0.01076	0.71307	70.361-9549.057	2.23 E-05 – 3.15E-05	95.34 – 99.64
Average	0.00657		5822.29	0.00216	98.53

The most elastic strain and stress were noticed respectively by the S4 and Node 1151. However, the least elastic strength was observed successively by Node 1151 and S6. Sample 4 has the most energy absorption with the elastic region. However, Node 1151 shown the least modulus of elasticity with an average modulus elasticity (mechanical and Abaqus) of 22E-04 Ksi. The overall confidence of the modulus resilience confidence was 98.53%.

Table 5.5 illustrates the ultimate stress-strain of the mechanical test and Abaqus simulation with Node 1151.

Table 5.5: Ultimate stress and strain with the compressive horizontal

Test	Strain (in/in)	Stress (Ksi)
Sample 4	0.0245	0.97149
Sample 5	0.02647	0.72352
Sample 6	0.002479282	0.71977
Abaqus N 1151	0.00007	1.3456
Range	0.00007-0.02647	0.71977-1.3456
Average	0.013379821	0.940095

The horizontal compressive test shows the most ultimate stress and strain with node1151 and S4. However, the least ultimate stress and strain were observed with S6 and Node 1151. The average maximum strain and stress were 00012% and 0.94Ksi. The node1151 was 28% high than S4 in strength.

The fracture point of Sample 1 was noticed at the strain 0.001286 % and the stress at a value 0.155154 Ksi. Figure 5.18 illustrates the energy absorbed at the plastic region of the sample.

5.2.1.2 The Modulus of Toughness

The modulus of toughness is the energy absorbed by the plastic region and was calculated by integrating the polynomial equation.

5.2.1.2.1 Sample 4

Figure 5.19 illustrates the modulus toughness of S4.

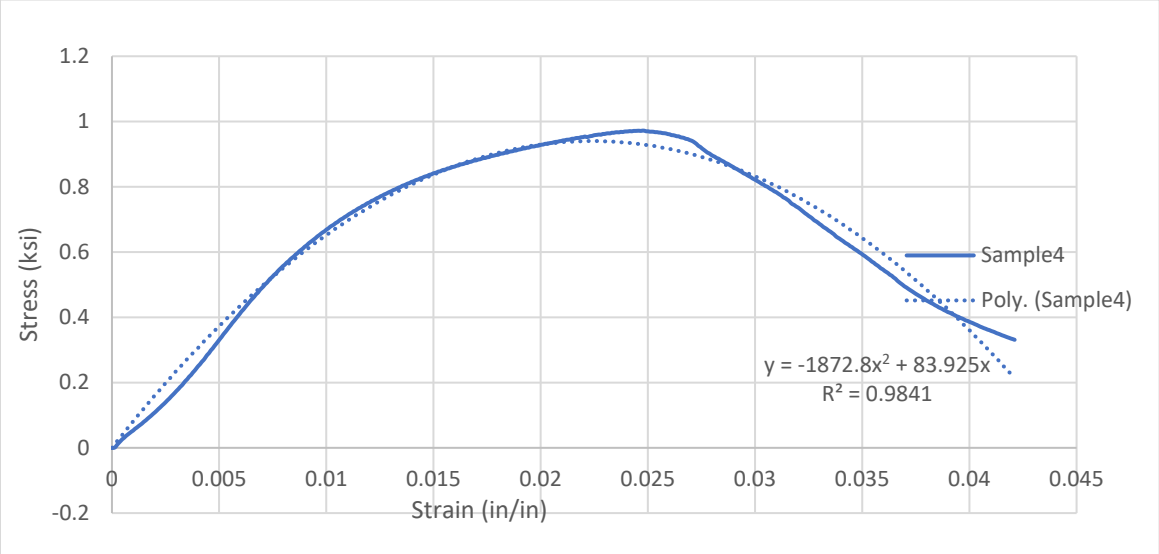

Figure 5.19: Modulus toughness of S4

The fracture strain and stress were 0.04211 % and 0.15516 Ksi. The modulus of toughness is defined by integrating the formula at the strain from 0 to 0.33102Ksi.

$$\int_0^{0.04211} Y(x)$$

$$\int_0^{0.04211} (-1872.8 * x^2 + 83.925 * x)\mathrm{d(x)}$$

$$\mathrm{Y(x)}=\left[-\frac{\mathrm{x}^2*(149824*\mathrm{x}-10071)}{240}\right]_0^{0.04211}$$

The modulus of the toughness of Sample 4 is 6.97485893×10−4 Ksi.

The same procedure was done with the S5, S6, and Node 1151.

5.2.1.2.2 Sample 5

Figure 5.20 illustrates the modulus toughness of S5.

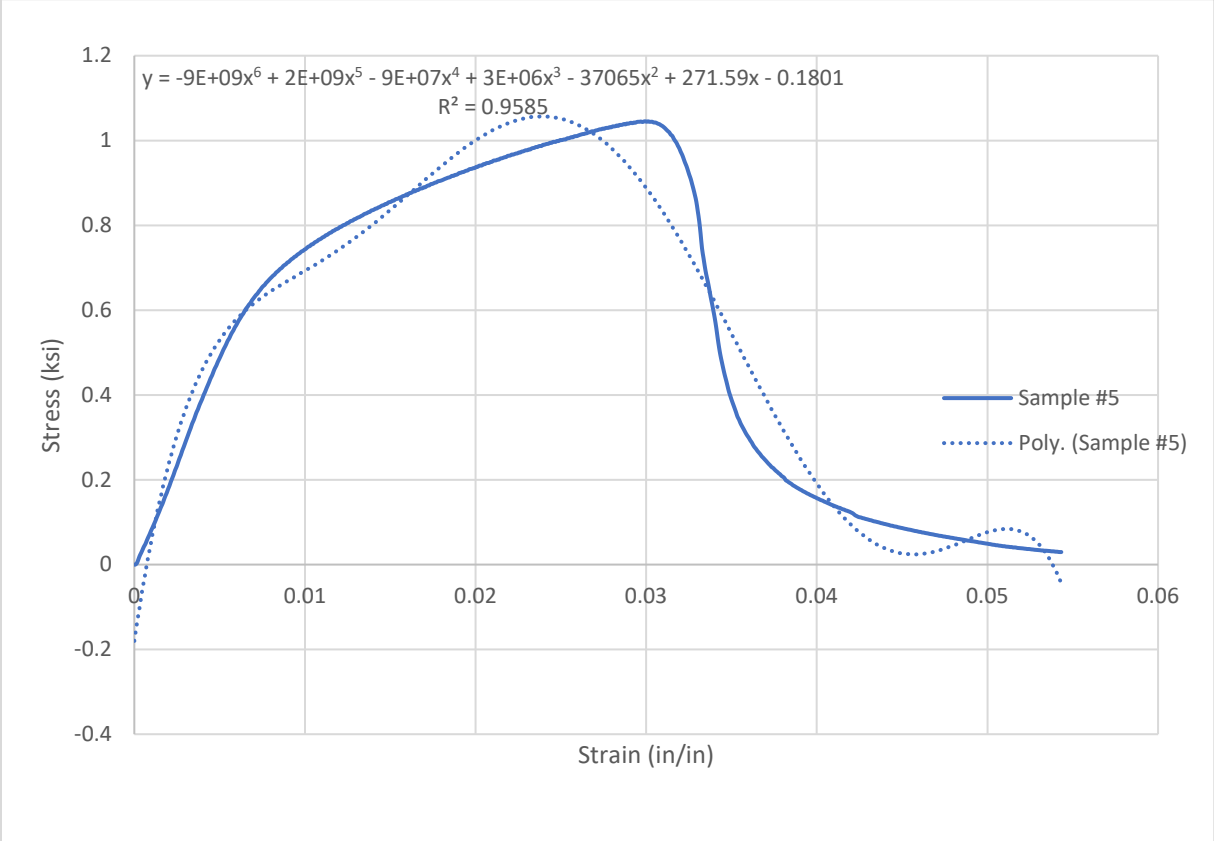

Figure 5.20: Modulus toughness of S5

The fracture strain and stress were observed at 0.05433% and 0.02955 Ksi. An exactness

of 95.85% from Eq. 5.19. The modulus of toughness was calculated by integrating Eq. 5.18 at the strain ranging from 0 to 0.05433%.

$$y = -9E+09*x^6 + 2E+09*x^5 - 9E+07*x^4 + 3E+06*x^3 - 37065*x^2 + 271.59*x - 0.1801 \quad \text{(Eq. 5.18)}$$

$$R^2 = 0.9585 \quad \text{(Eq. 5.19)}$$

The modulus of the toughness of Sample 5 is 2.80192026×10−4 Ksi.

5.2.1.2.3 Sample 6

Figure 5.21 illustrates the modulus toughness of S6.

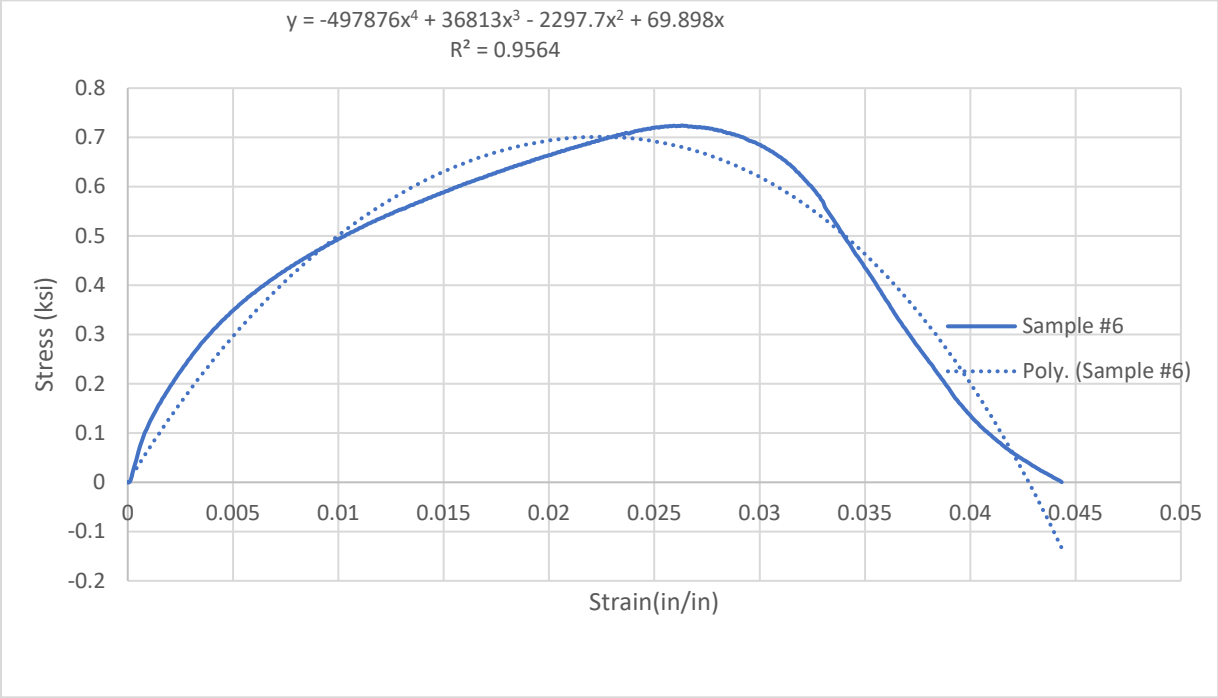

Figure 5.21: Modulus toughness of S6

The fracture strain and stress were respectively 0.04434% and 0.0029ksi. With an accuracy of 95.6% from Eq. 5.21. The modulus of toughness was calculated by integrating Eq. 5.20 at the strain array 0 to 0.04434%.

$$y = -497876x^4 + 36813x^3 - 2297.7x^2 + 69.898x \quad \text{(Eq. 5.20)}$$

$$R^2 = 0.95.6 \quad \text{(Eq. 5.21)}$$

The modulus of the toughness of Sample 6 is 6.2372987×10−4Ksi.

5.2.1.2.4 Abaqus Simulation with Node 1151

Figure 5.22 illustrates the modulus toughness of Node 1151.

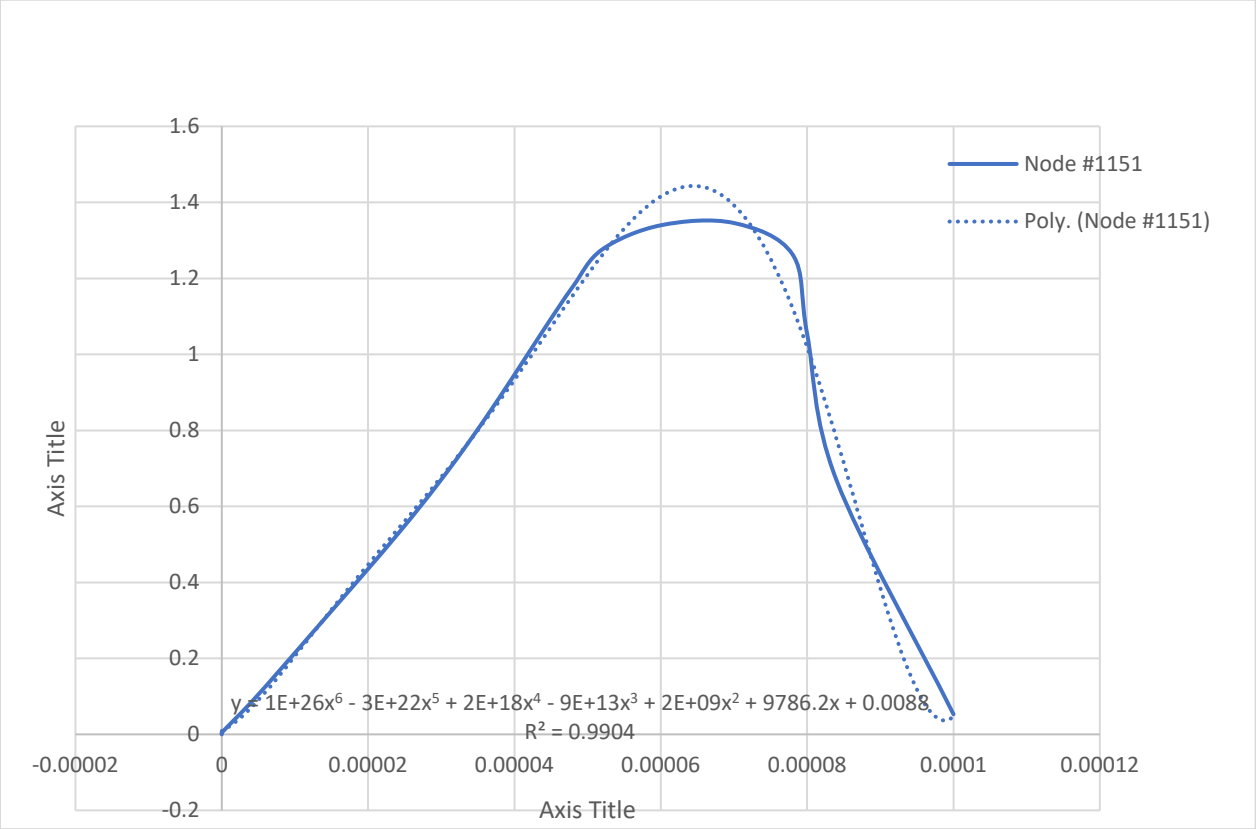

Figure 5.22: Modulus toughness of Node 1151

The plastic strain and stress located at 0.0001% and 0.0529ksi. An exactness of 99.04% from Eq. 5.23. The modulus of toughness was calculated by integrating Eq. 5.22 at the strain value from 0 to 0.04434% strain.

$$y = 1E+26x^6 - 3E+22x^5 + 2E+18x^4 - 9E+13x^3 + 2E+09x^2 + 9786.2x + 0.0088 \quad \text{(Eq. 5.22)}$$

$$R^2 = 0.9904 \quad \text{(Eq. 5.23)}$$

The modulus of the toughness of Node 1152 is 11.04950905×10−4Ksi.

The modulus toughness of the compressive vertical is illustrated in the Table 5.6.

Table 5.6: Modulus of the toughness of the compressive horizontal

Test	Fracture Strain (in/in)	Fracture Stress (Ksi)	Modulus of toughness (ksi)	Confidence (%)
Sample 4	0.04211	0.33102	6.97485893	98.39
Sample 5	0.05433	0.02955	2.80192026*E−4	95.85
Sample 6	0.04434	0.00029	6.2372987*E−4	95.6
Abaqus N 1151	0.0001	0.0529	11.049509052*E-4	99.04
Range	0.0001-0.0543	0.0029-0.0529	2.8*E-4 -11*E-4	95.6 -99.86
Average	0.03522	0.10344	6.765896736*E-4	97.22

The compressive horizontal of aluminum honeycomb sandwich noticed a fracture strength from 0.15Ksi to 0.17Ksi respectively with Node 1151 and S6. The fracture strain ranged from 0.0001 to 0 0.05433%, successively by Node 1151 and S5.

Abaqus simulation with the Node 1151 had the most modulus of toughness. However, Sample 5 had the least energy absorbed in the plastic region. Also, Node 1151 absorbed 36.8% more energy than Sample 4. The study of the modulus of toughness has 97% average confidence with the compressive horizontal.

Base on the test result with the horizontal compressive test, the aluminum honeycomb sandwich shows:

- No yield point for the four actual test data plots.
- Low modulus elasticity from 2.217 E-04 - 10.76 E-04 Ksi.
- Low modulus toughness from 2.217E-4 Ksi to– 10.76E-4 Ksi.
- Low fracture strain from 0.0001 -0.05433 below 5%
- A concentric crack propagation parallel at the stressed area of the samples from both tests (mechanical test and Abaqus simulation)

Therefore, we conclude that the aluminum honeycomb sandwich with the compressive

horizontal behaved like a brittle material.

5.3 Three-Point Bending Test of the Aluminum Honeycomb Sandwich

A 3-point bend of aluminum honeycomb sandwich loaded at the midsection of the part, both extremities pined at 1.5 inches from the edge. Therefore, the sample is placed horizontally across two supports. A force is applied to the midpoint causing a concave surface or a bend (V shape), forming a maximum deflection according to the load applied. Bending testing defines the material behavior (ductile or brutal material), the maximum deflection, and the ultimate moment location. It assumed that the material would fail under similar conditions when tested with a 3-point bend

The honeycomb sandwich three points bending tests from both simulation and experimental test illustrated that:

- A V shape was formed at the mid-section of the sample.
- The bottom layer noticed a tension pressure of the mi- section. However, the top layer had a V folding shape at the mid-section.
- The damage was concentric at the mid-section of the sample initiated by the pressure of the plumb.
- Honeycomb sandwich demonstrated a concentric crack propagation from both experimental and simulation test results. For illustration, refer to Figures 5.23 (mechanical test) and 5.24 (Abaqus simulation).

A 3-point bend of aluminum honeycomb sandwich loaded at the midsection of the part, both extremities pined at 1.5 inches from the edge. The maximum displacement was 1 inch. The seeding was performed at 0.2 inches.

Then the center of the top layer folded, and the bottom had tensile stress. Instigated by the load increases, the displacement rapidly increased, and fracture occurred immediately at the section's layers after the load reached its maximum value. The honeycomb layer exhibited linear

fracture, attributed to the load, density, and the sandwich fusion bond.

Bend 1 b- Bend 2

Figure 5.23: Mechanical test of the 3-point bend

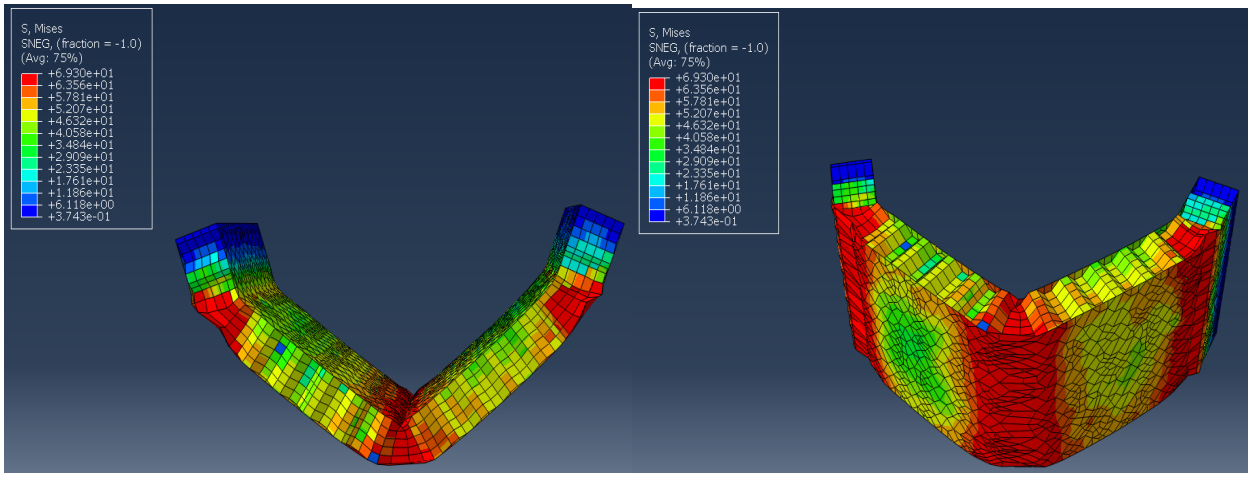

a- Abaqus Top view of 3-point bend b- Abaqus Bottom view 3-point bend

Figure 5.24: Abaqus simulation of the 3-point bend test

As the load increased, the displacement gradually enlarged, and local fracture of the cell wall began to occur immediately at the mid-section. When the load reached its maximum value, a crack was initiated. A repeated decrease peak load occurs with increasing displacement.

A fracture occurred at the model's midsection when the sample reached its maximum load, creating a decrease in load. Owing to the V shape formation due to concentric crack propagation by the continuous fracture of the cell wall, the final fracture occurred. The aluminum honeycomb

exhibited the brutal behavior of the aluminum.

The three plots of the 3-point bend of aluminum honeycomb sandwich illustrated the same tendency. The 3-point simulation test exposed the highest plot of the forces and displacement. The variances between real and predicted pore cells wall affected the aluminum sandwich's compressive test results from the disparity of the hexagonal distribution of the honeycomb's cell wall and each layer's density. For illustration, refer to Figure 5.23.

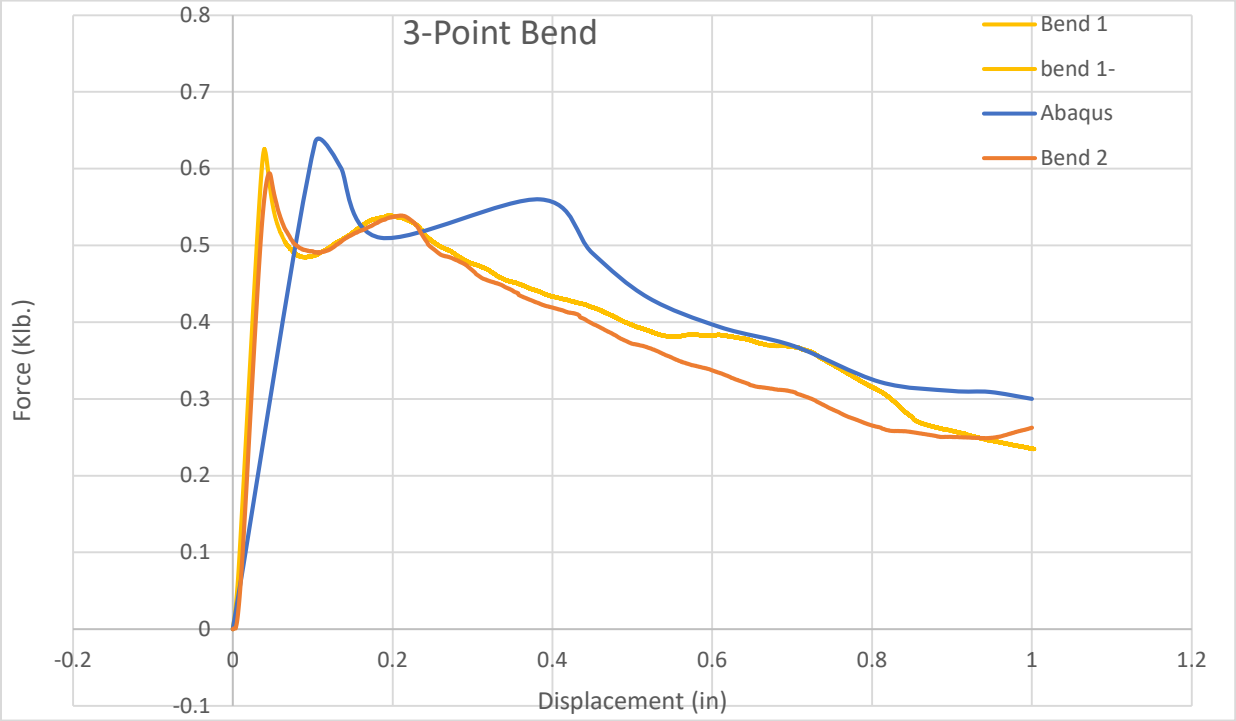

Figure 5.25: Plots with Abaqus and mechanical tests with compression horizontal

5.3.1 Maximum of Deflection of the Aluminum Honeycomb Sandwich 3-Point Bend

A supported aluminum honeycomb sandwich with a length of L=11.9 inches is carrying a load P at the sandwich's middle section. Eq. 5.24 represents the maximum deflection of the part.

$$P=\frac{48*E*I}{L^3}*\Delta max$$

$$K=\frac{48*E*I}{L^3}$$

By substation:

$$P=K*\Delta max$$

$$\Delta max=\frac{P}{K} \quad \text{(Eq. 5.24)}$$

where P is the load applied of the sandwich, K is the slope of the linear equation; E is the elastic modulus, I is the moment inertia, L is the length between two support, and Δmax is the maximum deflection.

5.3.1.1 Maximum of Deflection of the Bend Test 1

The displacement of the elastic region of Bend 1 is plotted by Figure 5.26.

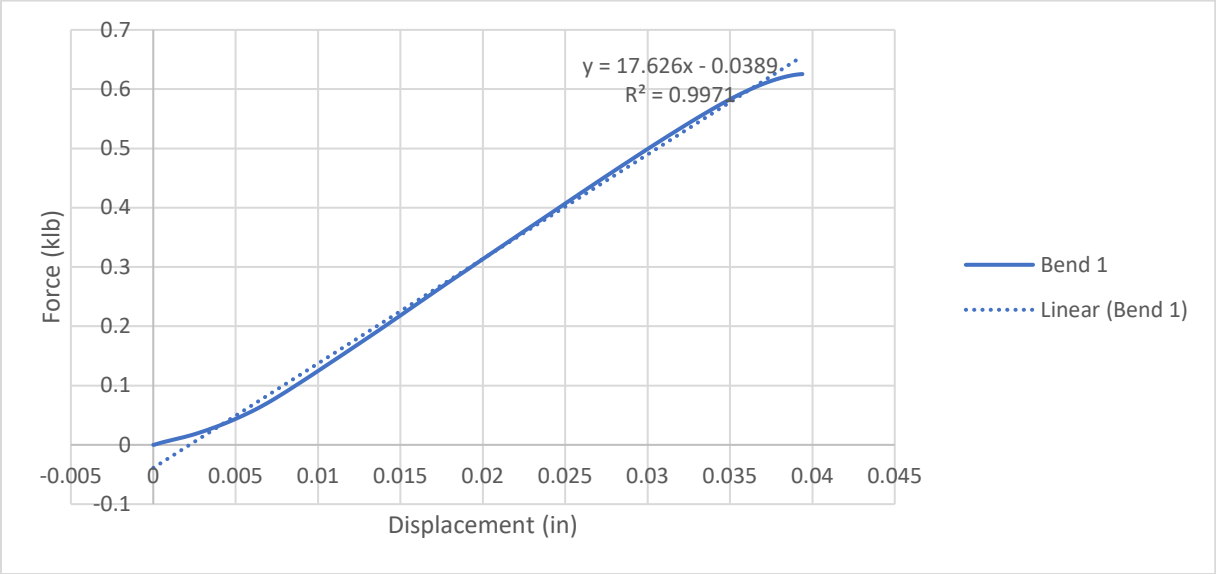

Figure 5.26: Bend 1 elastic displacement

Based on the formula, the coefficient of elasticity K_1 is the linear Eq. 5.25 which is equal to 17.626 Klb. The load factor and displacement were respectively 0.6255659 Klb and 0.03939632 in and the elastic.

$$y=17.626*x-0.0389 \quad \text{(Eq. 5.25)}$$

Therefore, the maximum deflection for the 3-point Bend Test 1 is:

$$\Delta max_1=\frac{P_1}{K_1}$$

$$\Delta max_1=0.6255659/17.626$$

The maximum deflection with the Bend Test 1 Δmax_1 is 0.035491inches.

The same procedure was done with Bend 2 and Abaqus simulation.

5.3.1.2 The Maximum Deflection of the Bend Test 2

The displacement of Bend 2 elastic regions is plotted by Figure 5.27.

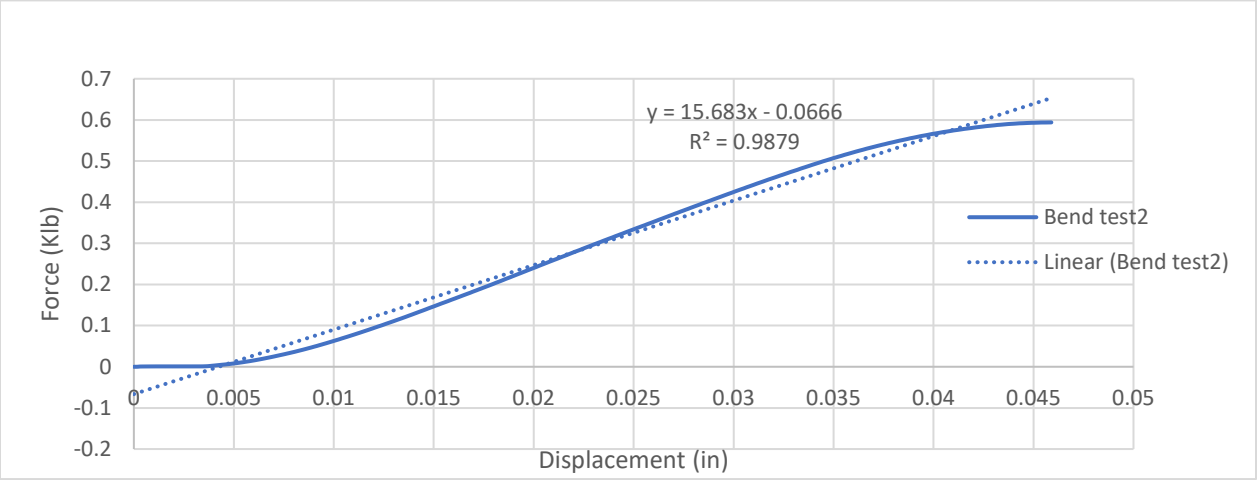

Figure 5.27: Bend 2 elastic displacement

Based on the formula, the coefficient of elasticity K is the linear Eq. 5.26 which is equal to 15.683 Klb. The load factor and displacement were respectively 0.5939427Klb and 0.04589108 inches.

$$y=15.683x-0.0666 \quad \text{(Eq. 5.26)}$$

The maximum deflection with Bend Test 2 Δmax_2 is 0.037872 in

5.3.1.3 The Maximum Deflection of the Abaqus Simulation Test

The displacement of the elastic region of the Abaqus simulation is plotted by Figure 5.28.

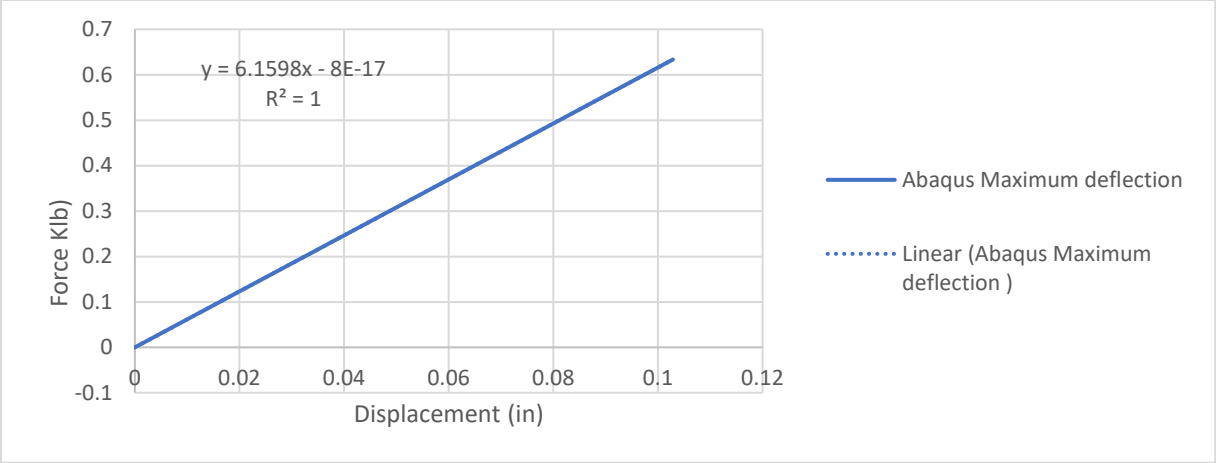

Figure 5.28: Abaqus simulation elastic displacement

Based on the formula, the coefficient of elasticity Ka is the linear Eq. 5.27 which is equal to 6.1598 Klb. The load factor and displacement were respectively 0.633637571 Klb, and 0.102866 inch.

$$y= 6.1598*x - 8E\text{-}17 \qquad \text{(Eq. 5.27)}$$

The maximum deflection with Abaqus simulation $\Delta max a$ is 0.102867in

The mechanical properties of the aluminum honeycomb sandwich with a 3-point bend test shown in Table 5.7.

Table 5.7: Mechanical properties of the 3-point data

Test	Force (Klb)	Strain (%)	Stress (ksi)	Displacement (in)	Maximum Deflection (in)
Abaqus	0.63364	10.5728	1.65704	1	0.10287
Bend 1	0.62557	10.4381	1.63593	1.00293	0.03787
Bend2	0.59394	10.4279	1.54657	1.00005	0.03549
Average	0.61772	10.4796	1.61318	1.001	0.058743
Range	0.5939-0.6336	9.3901-10.43809	1.414207-1.635933	1-1.002934	0.035-0.1

The study of the property's mechanical of the 3-point bend illustrated a concentric crack propagation. The maximum bending load ranged from 0.5939 Klb trough 0.6336Klb, respectively,

with the bend test1 and Abaqus simulation. The Abaqus simulation load factor rises 6% compared to Bend Test 2, and the Bend Test 1 rises 1%. The maximum displacement ranged from 0.035491 to 0.102867successively by Test 1 and the Abaqus.

5.3.2 Maximum Bending Moment and Shear Forces of the Aluminum Honeycomb Sandwich

Shear forces bending diagram used to analyze the aluminum honeycomb sandwich. When the sandwich is loaded, internal forces developed to maintain equilibrium. These internal forces are shear forces oriented to the vertical direction and regular forces oriented along the sandwich direction.

The bending moment and shear forces data define the internal forces developed when an external load P is applied to the sandwich. The FE has a concentric load at the midsection of the part and pinned supports.

The computerized MD Solid method is used for the analysis of the Mechanics of Materials. The sample's dimensions are 11.9 X 4 X 1 inch, both extremities pinned at 1.5 inches of length, and the pressure load applied at 5.95 inches. The thickness is 1 inch, and the Wight is 4 inches. Here the step involves each test result study with a length of 11.9inches.

The step of drawing the diagram of shear forces and bending moment are:

- First, a free body diagram is a draw.
- Then, use an equilibrium equation to calculate the reaction forces and moment.
- Furthermore, use the equilibrium equations to define the shear forces and bending moment diagram. This process is repeated for each test data.

When the sandwich is loaded, internal forces are developed to maintain equilibrium. These internal forces are shear forces oriented to the vertical direction and regular forces oriented along the sandwich direction. The analysis of the shear forces and bending moment was done base on the solid cross-section (without considering the porosity of the sandwich)

5.3.2.1 Analysis Maximum Bending Moment and Shear Forces with Abaqus:

A concentric load was applied at the midsection of the sandwich with an amplitude P= 633 lb. The analysis of aluminum honeycomb sandwich test 1 with MD Solid computerized method shows 320.2lb of shear forces and 1,409 lb.in bending moments. The diagram of loading shear forces and bending moment is illustrated in Figure 5.29.

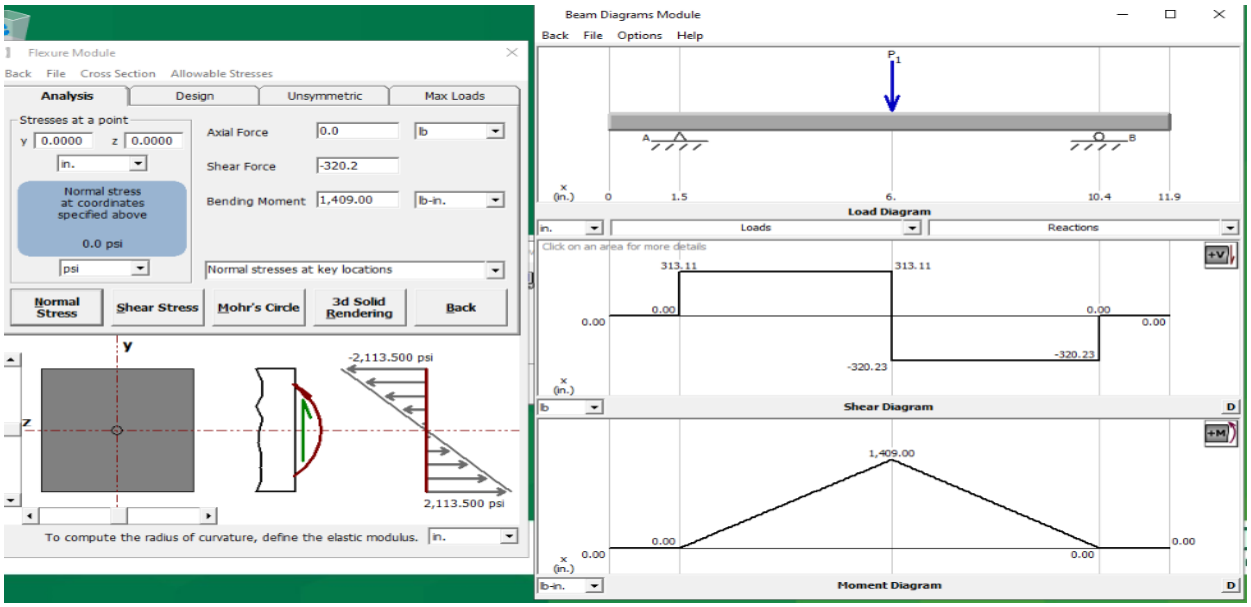

Figure 5.29: Analysis of shear forces and bending moment diagram in Abaqus

5.3.2.2 Analysis Maximum Bending Moment and Shear Forces of Bend Test 1

A concentric load was applied at the midsection of the sandwich with an amplitude P1= 625.57 lbs. The analysis of aluminum honeycomb sandwich test 1 with MB Solid computerized method shows 312.8 lb of shear forces and 1,391.87 lb.in bending moments. The diagram of loading shear forces and bending moment is illustrated with Figure 5.30

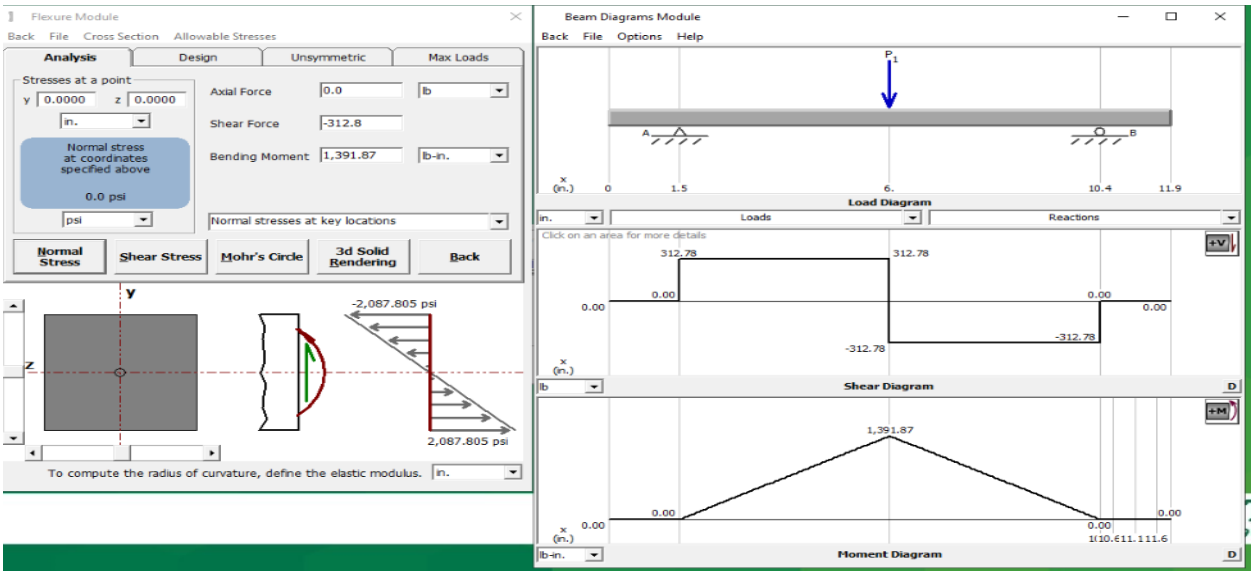

Figure 5.30: Analysis of shear forces and bending moment diagram with Bend Test 1

5.3.2.3 Analysis Maximum Bending Moment and Shear Forces of the Bend Test 2

A concentric load was applied at the midsection of the sandwich with an amplitude P= 593.4 lbs. The analysis of aluminum honeycomb sandwich test 2 with MB Solid method shows 296.97 lb of shear forces and 1,321.52 lb.in bending moments. The diagram of loading shear forces and bending moment is illustrated with Figure 5.31.

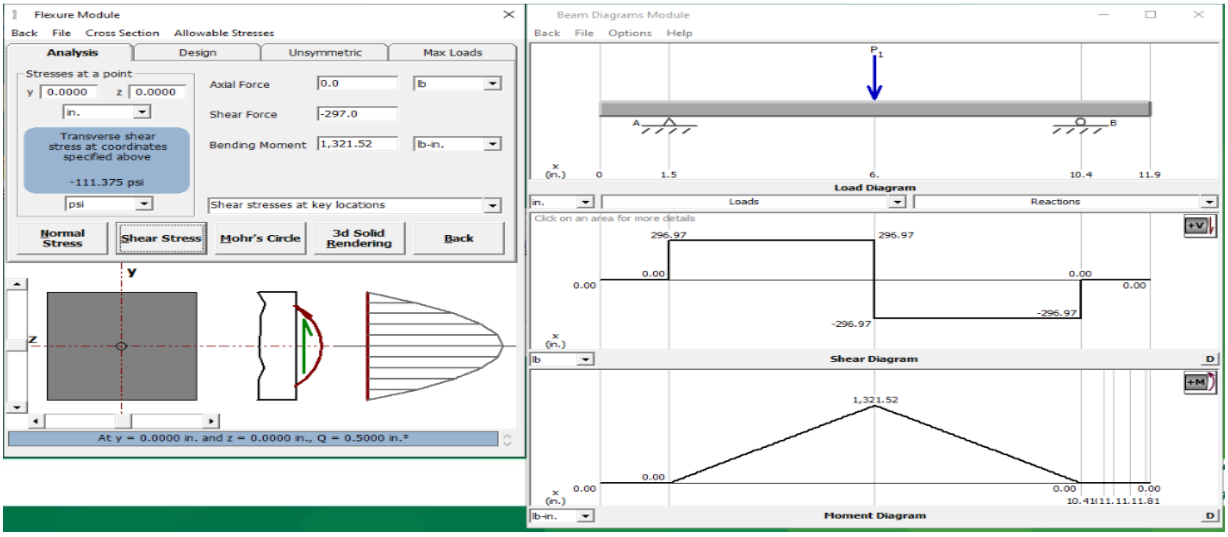

Figure 5.31: Analysis of shear forces and bending moment diagram with Bend Test 2

The maximum shear forces and bending moment, respectively shown in Table 5.8.

Table 5.8: Maximum shear forces and bending moment

Test	Shear Forces (Klb.)	Bending moment (Klb.in.)
Abaqus	0.3202	1.409
Bend 1	0.3128	1.39187
Bend2	0.297	1.32152
Average	0.31	1.37413
Range	0.297 to 0.32	1.32 to 1.41

The maximum displacement ranged from 0.035491 to 0.102867successively by Test 1 and the Abaqus. Both experimental and simulation result of the aluminum honeycomb sandwich shows:

- No actual yield point for three plot result.
- Have small data maximum of displacement oscillating from 0.035491-0.102867 in.
- A concentric crack propagation at the samples' midsection from both tests (mechanical test and Abaqus simulation).
- The shear forces ranged from 0.297 to 0.32 Klb.
- The bending moment ranged from 1.32 to 1.41 Klb.in.

The aluminum honeycomb sandwich with the 3-point test behaved like a brutal material

CHAPTER 6

CONCLUSION

The research contains three sets of results of the aluminum honeycomb sandwich: compression horizontal, compressive vertical, and bending tests. Also, each group was displayed mechanically and simulated in Abaqus. The mechanical properties include modulus of stress-strain, force, displacement, ultimate stress-strain, fracture point, density, poison ration, and the young modulus identified.

The FE energy absorbed defined, such as modulus of resilience and the modulus of toughness with the compression test. The maximum deflection, the shear forces, and bending moment were calculated for the 3-point bend test. The data result shows the behavior of the aluminum honeycomb sandwich.

Aluminum honeycomb sandwich behaved similarly to a brittle material in both the compressive vertical and horizontal test. Base on the view from the mechanical and Abaqus simulation, the crack propagation was concentric. The mechanical properties illustrated a low compressive strain below 5%. Without a visible yield point for the actual plot, result. A low modulus of resilience and toughness. The general study of modulus resilience and toughness confidence was above 95%.

Aluminum honeycomb behaved like a brittle component with the 3-point bend test. With a maximum displacement of 1 inch, the sandwich had a V-shaped image with the mechanical and the simulation test. The three tests show a concentric fracture area, no yield point, and a low maximum displacement. The average occupancy study of the maximum deflection was 99.5%.

Also, discrepancy of compressive result and 3-point bending test data between the mechanical and Abaqus simulation caused by:

- The contact with the aluminum honeycomb cell walls by deformation
- The thickness of the cells
- The distribution of the hexagonal cell
- The material's density
- The sandwich's fusion bonding

The work built a foundation for future research on application of aluminum honeycomb panels in building structures and portable shelters.

REFERENCES

[1] T. Dennis Claar et al (2000), Ultra-lightweight Aluminum Foam Materials for Automotive

[2] Advantages and Disadvantages of Hot Rolled Steel and Cold Rolled ... (2019-04-08) https://www.permanentsteel.com › news show › Advantages and Disadvantage...

[3] 10 things you need to know about aluminum honeycomb (8-7-2018). www.arrow-dragon.com › 10-things-you-need-to-kno...

[4] https://www.britannica.com/technology/aluminum-processing(1/23/2020),

[5] The Benefits of Aluminum Honeycomb in Aerospace (2/15/2017)

[6] https://www.buildsteel.org ›(January, 5, 2020), Framing Products Connections

[7] Yongyu Ye, et al. (2017), The applications of FEA in Proximal Humeral Fractures

[8] Abaqus – Wikipedia, https://en.wikipedia.org › wiki › Abaqus, (7/3/2010)

[9] P.S.Liu, G.F.Chen (2014), Special Porous Metal

[10] Ways Cold-Formed Steel Framing Can Lower Your Total Construction Costs https://www.reade.com › products › closed-cell-metal-foam

[11] H. Gravenkamp, et al. (2019), Critical assessment of different mass lumping schemes for higher-order serendipity FE

[12] T. Dennis Claar, Chin-Jye Yu, Ian Hall, John Banhart and Joachim Baumeister (2000), Ultra-lightweight Aluminum Foam Materials for Automotive Applications

[13] Padmanabhan Krishnan (2015), Introduction to Design with FE Approach and Applications

[14] https://informedinfrastructure.com/52155/how-steel-deck-is-shaking-up-cold-formed-steel-framing-design/ (1/24/2020)

[15] https://www.cfsteel.org/advantages-of-cold-formed-steel-framing, Advantages of Cold-Formed Steel Framing (1/23/2020)

[16] https://blog.framecad.com/blog/accelerate-the-construction-of-mid-rise-buildings-with-cold-formed-steel-and-framecad (1/23/2020),

[17] G.P. Thomas (2014), Aluminum Foam – Structure, Properties and Benefits

[18] Azom (2002), Aluminum, the History, Discovery and Development as a Product

[19] Bahar baştürk (2013), Development and Mechanical Behavior of FML/Aluminum Foam Sandwiches

[20] Fan Xinyua, et al. (2009), Modeling of Heat Conduction in Thermoplastic

[21] Jonas Grünewald, et al. (2015), Manufacturing of thermoplastic composite sandwich

[22] Vidyasagar Matta, et al. (2017), Flexural behavior of aluminum honeycomb sandwich core

[23] J. M. P. Martins, et al. (2016), Numerical modeling of the thermal contact in metal forming

[24] Catherine Amodeo, et al. (2017), FEA of Stress Intensity Factor Solutions for Discontinuous Gas Metal Arc Welds under Lap-Shear Loading Conditions

[25] Catherine Amodeo, et al. (2017), Application of Support Vector Machine and FEM to predict the mechanical properties of concrete

[26] M Sesha Reddy, et al. (2019), Application of FEM in Implant Dentistry

[27] Tao He et al. (2018), A smoothed FE approach for computational fluid dynamics:

[28] M Sesha Reddy, et al. (2019), Application of Finite Element Model in Implant Dentistry

[29] Tao He, et al. (2018), A smoothed FE approach for computational fluid dynamics: applications to incompressible flows and fluid–structure interaction

[30] K. K. Adewole, et al. (2015), FE failure analysis of wires for civil engineering applications with various crack-like laminations

[31] Houman Zahedmanesh, et al. (2012), A multiscale mechanobiological modelling framework using agent-based models and finite element analysis: application to vascular tissue engineering

[32] Sadeep Sasidharan, et al. (2019), Geometric Modification of a Switched Reluctance Motor for Minimization of Torque Ripple using FEA for Electric Vehicle Application.
[33] Ines Ivañez, et al. (2017) Compressive deformation and energy-absorption capability of aluminium honeycomb core

[34] Aluminium - Specifications, Properties, Classifications and ...www.azom.com (2005)

[35] Honeycomb structure – Wikipedia (2-2-2020).

[36] Most common uses of aluminum {5-9-2016)

[37] Jaroslav Kovacik, et al. (2018), Poisson's Raatio of closed-cell Aluminum Foams.

[38] Esther A. et al. (2012), Reconfiguration of a Milling Machine to Achieve Friction Stir